

MODELLING AND ANALYSIS OF HIERARCHICAL HONEYCOMB STRUCTURE USING FINITE ELEMENT METHOD

Thesis

Submitted to the



**G.B. Pant University of Agriculture & Technology,
Pantnagar-263145, Uttarakhand, India**

By

Mr. AMIT KUMAR SHAH

Id. No. 56993

**IN PARTIAL FULFILLMENT OF THE REQUIREMENTS
FOR THE DEGREE OF**

Master of Technology

In

Mechanical Engineering

(Design & Production Engineering)

October, 2022

ACKNOWLEDGEMENT

First of all, I bow my head before God who inspired me to face challenges of uneven times. All my sincere gratitude goes to him for the help he has given to me and his unfailing mercies over my life.

*I also express my deep sense of reverence and heartfelt gratitude to **Dr. Anadi Misra**, Professor, Department of Mechanical Engineering and Chairman of Advisory Committee for his guidance, constant encouragement, abundant counsel and his critical and constructive suggestions throughout the investigation. I am extremely indebted to him and wish to thank him from the bottom of the heart*

*With a profound sense of gratitude. I express warmest thanks to the members of the Advisory Committee, **Dr. Rakesh Saxena**, Professor, and Department of Mechanical Engineering. **Dr. V. K. Singh**, Professor, Department of Mechanical Engineering for their inspiring suggestions at every stage of this study. I sincerely thank **Dr. Kiran P. Raverkar**. Dean. College of Post Graduate Studies, **Dr. Alaknanda Ashok**, Dean, College of Technology, **Dr. Lokesh Varshney**, Head. Department of Mechanical Engineering, their keen interest in providing the necessary facilities*

I also express my sincere gratitude to all the faculty members of the Department of Mechanical Engineering for their continuous encouragement and wholehearted cooperation. I sincerely thanks to all the non- teaching staff members of the Department of Mechanical Engineering for their assistance and nice co-operation from time to time throughout.

*I owe a very special word of thanks to my mother **Mrs. Kusum Lata Shah**, my father **Mr. Hari Bhajan Shah**, my younger sister, **Kiran Shah**, and my friend, **Mridula**, for their boundless, generosity, everlasting inspiration, blessing abundant love and affection throughout. This thesis is heartily dedicated to my brother, **Himanshu Shah**, who is always with me as blessings. Appreciations are also extended to my seniors, juniors, and friends especially to **Nagendra Kumar**, **Avichal Pandey**, **Rakesh Chandra**, **Rahul Pant**, **Gauray Prakash Joshi**, **Rajat Pant**, **Tarun Bhatt**, **Nikhilesh Singh Bisht**, **Pankaj Kumar** and **Prem Kumar**, for their encouragement and helping hands at various stages of the work. This list is obviously incomplete but allows me to submit and I once again my heartfelt gratitude to all those who helped me directly or indirectly in this work.*



Place: Pantnagar
October, 2022

(**Amit Kumar Shah**)
Author

CERTIFICATE – I

This is to certify that the thesis entitled “**Modelling and Analysis of Hierarchical Honeycomb Structure using Finite Element Method**” submitted in partial fulfilment of the requirements for the degree of **Master of Technology in Mechanical Engineering** with major in **Design and Production Engineering** of College of Post-Graduate Studies, G.B. Pant University of Agriculture & Technology, Pantnagar, is a record of *bonafide* research carried out by **Mr. Amit Kumar Shah**, ID. No. **56993** under my supervision and no part of the thesis has been submitted for any other degree or diploma.

The assistance and help received during the course of this investigation have been acknowledged.

Pantnagar
October, 2022



(Anadi Misra)
Chairman
Advisory Committee

CERTIFICATE– II

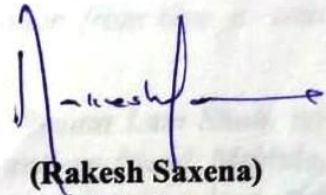
We, the undersigned, members of the Advisory Committee of **Mr. Amit Kumar Shah**, ID. No. **56993**, a candidate for the degree of **Master of Technology in Mechanical Engineering** with major in **Design and Production Engineering** agree that the thesis entitled **“Modelling and Analysis of Hierarchical Honeycomb Structure using Finite Element Method”** may be submitted in partial fulfilment of the requirements for the degree.



(Anadi Misra)
Chairman
Advisory Committee



(V.K. Singh)
Member



(Rakesh Saxena)
Member

TABLE OF CONTENTS

LIST OF TABLES

LIST OF FIGURES

LIST OF ABBREVIATIONS

LIST OF SYMBOLS

S.No.	CHAPTER	Page No.
1.	INTRODUCTION	1-15
1.1	General	1
1.2	Cellular solids and its making	2
1.2.1	Honeycombs	2
1.2.2	Forms	3
1.3	Honeycomb composite structures	3
1.4	Component of honeycomb sandwich panel	5
1.4.1	Face sheet	5
1.4.2	Core	6
1.4.3	Adhesives	6
1.5	Manufacturing Methods	6
1.6	Honeycomb Materials	8
1.7	Cell Configuration	9
1.8	Honeycomb property and application	10
1.9	Failure Modes of Honeycomb Structure	11
1.10	Hierarchical Honeycomb	14
1.11	Aim of Thesis	14
1.12	Thesis Outline	14
2.	REVIEW OF LITERATURE	16-26
2.1	General	16
2.2	Analysis of Geometry Change	16
2.3	Analysis of Hierarchical structure	21
2.4	Research Gap	25

2.5	Objective	26
3.	MATERIALS AND METHODS	27-38
3.1	General	27
3.2	Density of Hexagonal cell	27
3.3	Deformation Mechanism in Honeycomb core	28
	3.3.1 In-plane Deformation	29
	3.3.2 Out-of-plane deformation	29
3.4	Properties of honeycomb cell	30
	3.4.1 In-plane properties	31
	3.4.2 Out-of-plane properties	32
3.5	Bending energy due to crushing	34
3.6	Sub-structure (α) and super-structure factor (β)	34
3.7	Modelling and FEM of sub-structure and super-structure using ANSYS	34
	3.7.1 Structural modeling	35
	3.7.2 Static structure module	35
	3.7.3 Element type and Mesh size	36
	3.7.4 Material model	37
	3.7.5 Boundary conditions	37
	3.7.6 Solver outcome	38
4.	RESULTS AND DISCUSSIONS	39-56
4.1	Introduction	39
4.2	Validation using Finite Element Method	39
4.3	Mesh convergence test	40
4.4	Effect of super-structure	41
	4.4.1 Adjacent pattern	41
	4.4.2 Alternate pattern	44
	4.4.3 Face sheet thickness variation	47

4.4.4	Super-structure wall thickness variation	54
5.	SUMMARY AND CONCLUSIONS	57-58
5.1	General	
5.2	Future Scope	
	LITERATURE CITED	
	CURRICULUM VITAE	
	ABSTRACTS	

LIST OF TABLES

Table No.	Title	Page No.
3.1	Mechanical properties of material used.	37

LIST OF FIGURES

Figure No.	Title	Page No.
1.1	Microstructure of the investigated honeycomb	3
1.2	Microstructure of the investigated foam sheet	3
1.3	Honeycomb sandwich structure	4
1.4	(a) Manufacturing process of Honeycomb core using expansion method; (b) Manufacturing process of Honeycomb core using corrugation method	7
1.5	Manufacturing of Honeycomb core using 3D printer	8
1.6	Honeycomb cell configurations	10
1.7	Comparative sonic fatigue resistance of conventional and sandwich structures	11
1.8	(a) Facing failure; (b) Transverse shear failure; (c) Flexural crushing of core; (d) Local crushing of core; (e) General buckling; (f) Shear crimping; (g) Face wrinkling (core) and face wrinkling (adhesive); (h) Intracell buckling (dimpling)	13
3.1	Hexagonal honeycomb unit cell	27
3.2	Hexagonal honeycomb core with in-plane loading on plane X_1 - X_2 and out-of-plane loading on plane normal to X_3	28
3.3	In-plane deformation of honeycomb (a) an un-deformed honeycomb; (b) yielding of cell walls in X_1 direction (compression); (c) yielding of cell walls in X_2 direction (compression)	29
3.4	Cell deformation due to elastic compression: (a) un-deformed honeycomb; (b) & (c) bending caused by loads in X_1 and X_2 directions	30
3.5	In-plane loading of honeycomb core	31
3.6	Cell wall bending and rotation due to linear elastic shear: (a) un-deformed honeycomb (b) displacement and rotation due	32

	to shear stress	
3.7	Out-of-plane loading of honeycomb core	32
3.8	(a) honeycomb carrying loads on the faces normal to X_3 ; (b) one cell showing walls a, b, c	33
3.9	(a) Unit cell with 1 st order sub-structure hierarchy; (b) Unit cell with 1 st order super-structure hierarchy.	34
3.10	Modelling of structure using SolidWorks.	36
3.11	Interface of project schematic window in ANSYS.	36
3.12	Boundary conditions for honeycomb sandwich structure.	38
4.1	Fig. 4.1 Validation of experimental results with numerical results	39
4.2	Mesh convergence test performed in ANSYS.	40
4.3	(a) Placement of super-structure in adjacent pattern; (b) Placement of super-structure in alternate pattern.	41
4.4	Boundary conditions for super-structure with adjacent pattern honeycomb sandwich.	41
4.5	Deflection as output for super-structure with adjacent pattern honeycomb sandwich.	42
4.6	Force vs. Displacement graph with cell height of 10mm.	42
4.7	Force vs. Displacement graph with cell height of 13.5 mm.	43
4.8	Force vs. Displacement graph with cell height of 15 mm.	43
4.9	Boundary conditions for super-structure with alternate pattern honeycomb sandwich.	44
4.10	Deflection as output for super-structure with alternate pattern honeycomb sandwich.	45
4.11	Force vs. Displacement graph with cell height of 10mm.	45
4.12	Force vs. Displacement graph with cell height of 13.5 mm.	46
4.13	Force vs. Displacement graph with cell height of 15 mm.	46
4.14	(a) Sandwich structure with core height of 13.5 mm and face sheet height with 0.25 mm each; (b) Sandwich structure with core height of 13.5 mm and face sheet height with 0.50 mm each; (c) Sandwich structure with core height of 13.5 mm	47

	and face sheet height with 0.75 mm each.	
4.15	Force vs. Displacement graph with cell length as 4.36 mm and cell height as 10 mm.	48
4.16	Force vs. Displacement graph with cell length as 5.32 mm and cell height as 10 mm.	48
4.17	Force vs. Displacement graph with cell length as 6.28 mm and cell height as 10 mm.	49
4.18	Force vs. Displacement graph with cell length as 7.14 mm and cell height as 10 mm.	49
4.19	Force vs. Displacement graph with cell length as 4.36 mm and cell height as 13.5 mm.	50
4.20	Force vs. Displacement graph with cell length as 5.32 mm and cell height as 13.5 mm.	50
4.21	Force vs. Displacement graph with cell length as 6.28 mm and cell height as 13.5 mm.	51
4.22	Force vs. Displacement graph with cell length as 7.14 mm and cell height as 13.5 mm.	51
4.23	Force vs. Displacement graph with cell length as 4.36 mm and cell height as 15 mm.	52
4.24	Force vs. Displacement graph with cell length as 5.32 mm and cell height as 15 mm.	52
4.25	Force vs. Displacement graph with cell length as 6.28 mm and cell height as 15 mm.	53
4.26	Force vs. Displacement graph with cell length as 7.14 mm and cell height as 15 mm.	53
4.27	(a) Super-structure cell wall thickness as 0.32mm; (b) Super-structure cell wall thickness as 0.64mm	54
4.28	Force vs. Displacement graph with cell length as 4.36 mm and cell height as 13.5 mm.	55
4.29	Force vs. Displacement graph with cell length as 5.32 mm and cell height as 13.5 mm.	55

LIST OF ABBREVIATIONS

Abbreviation	Full Form
ρ	: Density in Kg/m ³
α	: Sub-structure size factor
β	: Super-structure size factor
σ	: Stress in MPa
L	: Length
W	: Width
T	: Thickness
FEA	: Finite Element Analysis
FEM	: Finite Element Method
ABS	: Acrylonitrile Butadiene Styrene
PLA	: Polylactic Acid
Al	: Aluminium
E	: Young's Modulus
vs.	: Verses
N	: Newton
<i>et al.</i>	: and others
etc.	: Etcetera
HOBE	: Honeycomb before expansion
K	: Kelvin

LIST OF SYMBOLS

Symbol		Meaning
>	:	Greater than
%	:	Percent
/	:	per
<	:	Less than
Σ	:	Summation
\leq	:	Less than or equal to
\geq	:	Greater than or equal to
$^{\circ}\text{C}$:	degree Celsius
$^{\circ}\text{F}$:	degree Fahrenheit
mm	:	Millimeter
\approx	:	Almost equal to
$\sqrt{\quad}$:	Square root
dB	:	decibel



Introduction



Chapter 1

INTRODUCTION

1.1 General

Material is an important element in product design and the amount of material used is highly impacted by the product's structure. The structures employed in today's situation overcompensate for the items' load-bearing requirements. Therefore, numerous typical architectures are developed to optimize material choices in order to get significant outcomes. Many applications of such hollowed structures over solid-profiled structures are dependent on a variety of variables, including stress distribution, deformation, manufacturability etc. Biological structures which are 2-D cellular materials like bee hives, the microstructure of abalone shells and bamboo cross-sections served as inspiration for the regular periodic microstructure of honeycombs. This significant reduction in modelling and analysis work is achieved when flawless in-plane isotropy is performed using honeycombs with uniform hexagonal cells (**Gibson and Ashby 1997**).

The first sandwich panel for an aeroplane was created in 1919, utilizing end-grain balsa wood as the core and thin mahogany facings as the faces. It served as the main support for a seaplane's pontoons. Later during World Wars I and II, the main construction of Italian sea-planes was made of plywood skins adhered to a balsa wood core. These aircraft were flown in full squadrons to Brazil in the 1920s and to the Chicago World's Fair in the 1930s, which is a truly amazing indication of flight time for the time. The A380 and 787 are two of Airbus and Boeing's most recent commercial aircraft designs, which demonstrate the progression of composite material utilization. Compared to the Airbus A340 which was introduced in 2002, the Airbus A380's primary structure has 25% Carbon Fiber Reinforced Plastic (CFRP) structures.

As time goes on, the need for even small armies to be completely armored became apparent during the early stages of the industrial revolution and the experience of ever growing dangers. It was decided that ballistic protection was necessary. Later, military and paramilitary activities became even more technologically advanced. They adopted highly technological warfare and munitions strategies. This increased the need for better armor materials. The armor must be lighter, more damage resistant, flexible, and highly energy absorbent. Now composite materials that enable large-scale production are gaining

attention. Variety of reinforcing components and the development of novel processing are available. There are now several studies looking into ways to enhance the performance of composite structures. To enhance the energy-absorbing qualities of the structures without losing sight of the total weight, researchers are examining alternative settings for sandwich composite materials. Other parameters that may be changed to enhance the performance of sandwich composite structures include material qualities, thickness, and core characteristics.

1.2 Cellular Solids and its making

A cellular solid is made up of a network of connected solid struts or plates that act as cell boundaries and faces. The relative density of a cellular solid is its most important factor.

$$\text{Relative density } \left(\frac{\rho^*}{\rho_s} \right) = \frac{\text{Density of cellular material } (\rho^*)}{\text{Density of solid from which the cell walls are made } (\rho_s)} \quad (1.1)$$

It is possible to create specialized ultra-low-density foams with a relative density as low as 0.001. The relative densities of most softwoods range from 0.15 to 0.40. Cork is roughly 0.14. Polymeric foams used for insulation, packing, and cushioning are typically between 0.05 and 0.2. As the relative density rises, cell walls thicken and pore space decreases (**Gibson and Ashby 1997**).

Polymers are the most popular among all cellular. However, cells may be made from metals, ceramics, glasses, and even composite materials. Cellular solids are primarily divided into:

- a) Honeycomb
- b) Forms

1.2.1 Honeycombs

A honeycomb is a structure made up of hexagonal prismatic cells. Honeycomb cell axes are always approximately horizontal, with the open end being higher than the rear end.

The most apparent method is to form sheet material into a half hexagonal shape and then glue the corrugated sheets together. Another method through which paper-resin honeycombs are made is extrusion.

In this method, glue is applied in parallel strips to a flat sheet, then the sheets are stacked such that the adhesive holds them together. Sheets are then pulled apart to form a honeycomb shape. The microstructure of honeycomb is depicted in Fig. 1.1 below.

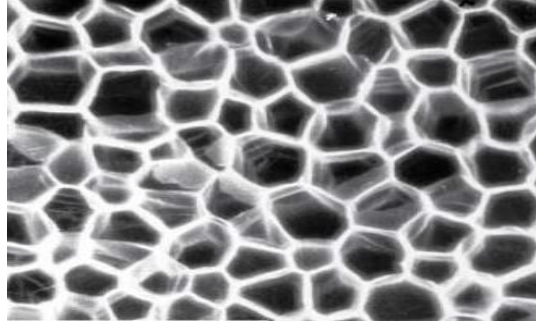


Fig.1.1 Microstructure of the investigated honeycomb (Gibson and Ashby 1997).

1.2.2 Forms

Different procedures are utilised to create various kinds of solids. By adding gas bubbles to the heated or liquid polymer, bubbles are allowed to expand and stabilize. After that, when cross-linking or chilling of the entire mixture happens, polymers are foamed. Thus foams are substances created when pockets of gas are trapped in a liquid or solid. The majority of foams have substantial gas volumes with thin coatings of liquid or solid separating the gas regions. The microstructure of honeycomb is depicted in Fig. 1.2 below.

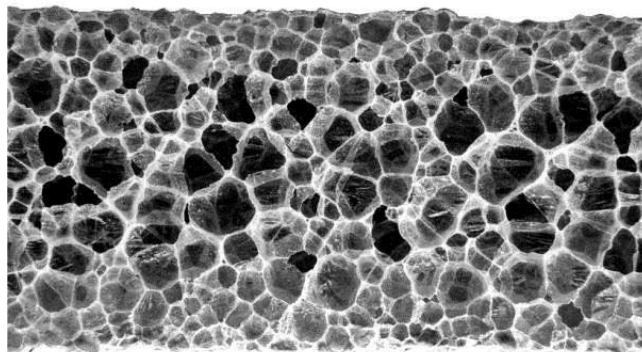


Fig.1.2 Microstructure of the investigated foam sheet (Gibson and Ashby 1997).

1.3 Honeycomb Composite Structures

A honeycomb is made of many open cells that are created by connecting a lot of very thin sheets of material. The cells often form hexagons. Sandwich structures are layered laminated panel structures with light-weight cores and thin face sheets attached.

This composite construction is very stiff, strong and outstanding thermal insulation. A number of other advantages over monolithic metals are that such structures are frequently used in weight-critical industries such as aerospace, automotive, marine, in fields of architecture, transportation, mechanical engineering, chemical engineering, biomedicine, and many others. Natural honeycomb structures have served as an inspiration for the creation of low density, high stiffness structures (**Bitzer 1997**).

Figure 1.3 depicts the honeycomb sandwich construction. Sandwich composite constructions with a honeycomb structure provide great strength, low density, and high impact-absorbing capabilities. According to research, honeycomb structures exhibit great stiffness and strength when loaded in an out-of-plane orientation because the deformations requires axial extension or compression of strong cell walls.

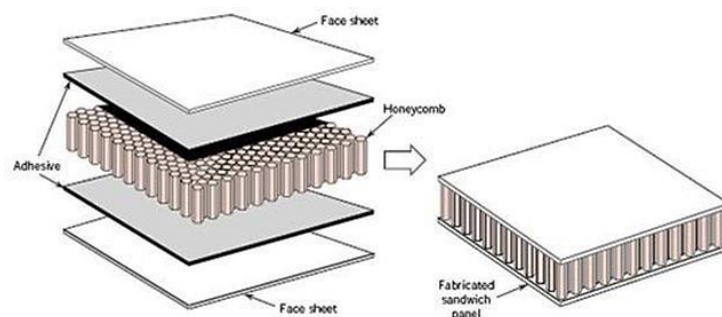


Fig.1.3 Honeycomb sandwich structure (Bitzer 1997)

Creating a plate like assembly with artificial honeycomb structures by layering a honeycomb material between two thin layers that give strength in tension is a typical method. The tremendous strength of honeycomb materials makes them suitable for applications requiring flat or slightly curved surfaces. For this reason, they are frequently employed in the aerospace sectors. Materials including aluminium, fiberglass, and advanced composites have been used in aeroplanes and rockets since the early 1950s.

In many packaging industries, packaging materials like cardboard with a honeycomb structure made of paper have been introduced. In recreational items like skis and snowboards, the honeycomb structure may be seen. The primary application of honeycomb is in structural design. The most fundamental and typical cellular honeycomb configuration is the classic hexagonal honeycomb.

The principal applications for honeycomb structures are in the aerospace and aviation industries, as well as in the maritime, high-speed rail, automobile, industrial construction, mantle, and packaging sectors. It is also utilised in the furniture industry, in sports equipment, for doors, in architectural projects, and for decorating caravans, boats, and yachts. Honeycomb sandwich structures are used in energy absorption for buffer designs to reduce the loss of life and property after collisions involving large vehicles. Honeycomb structures are widely employed in road barriers to reduce the risk of accidents on the steep bends of highway overpasses. Other uses for honeycomb include energy absorption, directionality of the air, thermal panels, acoustic panels, light diffusion and radio frequency shielding,

To avoid unanticipated outcomes in engineering construction it is vital to understand about the material's mechanical behaviour. Especially in the case of production, installation, and usage against any external impact. The energy absorption characteristics of honeycomb composites under strength, fracture, deformation values and impact loading may be discovered by impact testing.

1.4 Components of honeycomb sandwich panel

Three components including two face sheets, a core, and adhesive layers make up each honeycomb panel. Each has a sizable impact on the mechanical characteristics of the honeycomb panel.

1.4.1 Face sheet

Face sheets bear nearly all of the bending and in-plane stresses. They also specify flexural stiffness, as well as out-of-plane shear and compressive behaviour. Because the facings are designed to provide nearly all of the tension, compression or bending resistance, they should be moderately dense. They must be kept at suitable distance from mid-plane of sandwich panel. The skin's layup and thickness must be customized to fit the unique needs. Therefore, face sheets constructed with adequate out-of-plane rigidity and in-plane stiffness are important. The facings' thickness and layup must be planned to satisfy the specific criteria.

1.4.2 Core

The main goal of the core is to reduce weight while increasing the flexural stiffness of the entire structure. The face sheets and core interface are usually the weakest components of a sandwich panel, therefore low density core material is introduced. Core is crucial in providing strong shear resistance and stabilizing. Core and face sheet must have good surface finish to improve adhesive bonding. Both anisotropic honeycomb and isotropic foam are popular options for the core materials. Cores are primarily used in sandwich composites for load-carrying reasons in aerospace, aeronautics, marine vehicles, transportation, and military applications due to their light-weight, specific bending rigidity, and strength under dispersed loads.

1.4.3 Adhesives

It is crucial to choose the right adhesive for bonding. Adhesives are the bonding agent that holds the face sheet and core material of a honeycomb sandwich construction together. The adhesive substance must possess mechanical qualities that are on par with or even superior than those of the core substance.

Debonding is not permitted since the failure of the sandwich panel cannot be attributed to the failure of adhesive seams. Among the several adhesive alternatives, PU (Polyurethane) adhesives are the most typically utilised in large numbers. The curing of the adhesive is regulated by factors such as humidity, pressure, and temperature. The most common adhesive is a combination of a base resin (polyol) and a curing agent (isocyanate). There are also thermally activated solid adhesive films that eliminate glue waste and have manufacturer-guaranteed qualities (**Bishopp 2011**).

1.5 Manufacturing method

Adhesive bonding, resistance welding, brazing, diffusion bonding, and thermal fusion are the five fundamental processes used to create honeycomb. These techniques are based on the connections between the nodes. Adhesive bonding is by far the most used manufacturing procedure. It is conceivable that 95% of honeycomb cores are made in this technique. A polyimide node adhesive has a maximum operating temperature of roughly 750 °F (399°C) for adhesively attached nodes (**Bitzer 1997**).

The expansion process and the corrugation process are two well-known ways to transform sheet material into honeycomb. The expansion procedure entails initially adhering layers of materials with printed sticky lines together. The block, which is made up of a few layers of that substance is then divided into pieces according to their sizes. After each piece has been stretched, multiple honeycomb cores are obtained. In the corrugation process, the material is first corrugated or folded into a certain form before the shaped layers are adhered to create a honeycomb block. The block may then be cut into pieces that are the right size. Figures 1.4(a) and 1.4(b) make it simpler to understand both procedures.

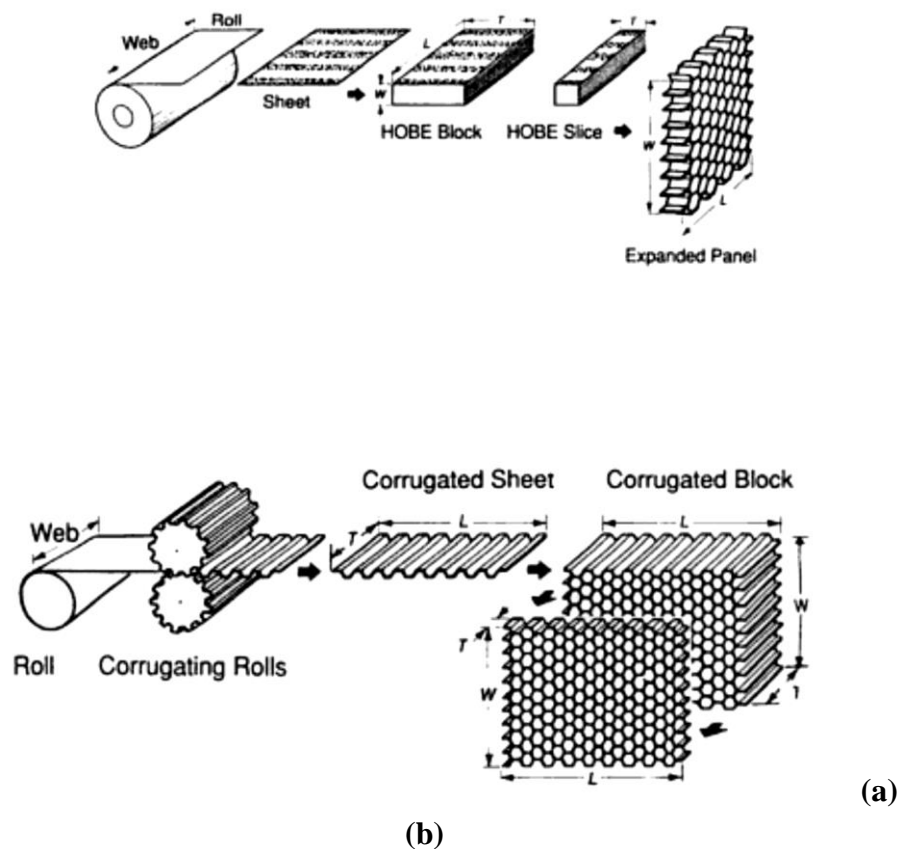


Fig.1.4 (a) Manufacturing process of Honeycomb core using expansion method
(b) Manufacturing process of Honeycomb core using corrugation method
(Bitzer 1997)

The five steps of the expansion process are roll, sheet, HOBE block (honeycomb before expansion), HOBE slice, and enlarged honeycomb panel. Rolls, corrugating rolls, corrugated sheets, corrugated blocks, and honeycomb panels are all components of the corrugation manufacturing process. Nomex honeycomb is produced using a different method. There, the expansion manufacturing process is the foundation. The procedure begins by adhering layers of material with printed adhesive lines together, just like the conventional expansion production method. These bonded layers are then stretched into a honeycomb block, which is then warmed to maintain its form. The block is heated in the oven after being repeatedly submerged in phenolic resin so that the resin may cure. The result is a block of Nomex honeycomb that may be machined or cut into the desired form.

The new technology of 3D printed structures is gaining popularity right now since it allows for speedier construction, cheaper labor, and less waste to be created. Considering strength and stiffness are two of the most important design criteria, 3D printing honeycomb structures enables for weight reduction without losing either. The honeycomb core created using a 3D printer is shown in the Fig. 1.5 below.

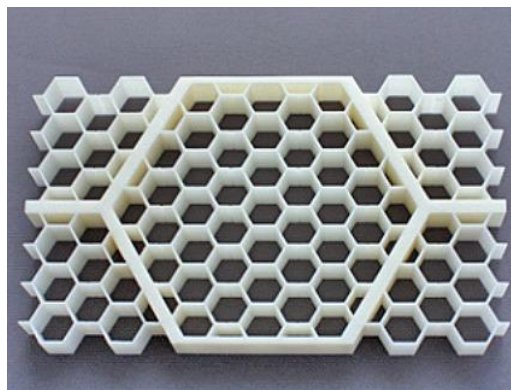


Fig.1.5 Manufacturing of Honeycomb core using 3D printer

1.6 Honeycomb Material

Manufacturers have several challenges, such as difficulty in simulating the massive hexagonal core and the complicated geometry of the core. So, core material must be substituted with a simple equivalent volume with elastic orthotropic qualities. It is important to choose a material for the honeycomb core that will provide benefits including superior mechanical characteristics, great crushing qualities, tiny cross-section regions, and big exposed area inside cells.

Honeycomb structure is influenced by the material, cell size, cell wall thickness, and bulk density of a regular hexagonal cell. The three major building materials are aluminium, glass fiber reinforced plastic, and aramid paper. Among these, engineering applications frequently employ aluminium honeycomb and aramid paper (Nomex™) honeycomb.

Aluminium honeycomb sandwich constructions are structurally remarkably efficient. Still their use in the aerospace industry is currently restricted because they are vulnerable to long-term moisture exposure, which can result in corrosion. They may undergo adhesive bond weakening and significant face sheet debonding. This deterioration has led to a number of in-flight malfunctions, panel failures during repairs, and an increase in the maintenance workload required to diagnose and fix issues.

Since honeycomb is an anisotropic material, its shear characteristics change depending on whether the sheet is tested along its length or across its breadth. The construction of honeycomb materials involves creating ribbons with a semi-hexagonal profile and joining them in pairs to create hexagonal cells. The honeycomb made from these ribbons has double walls on two sides of each unit cell, giving the plane characteristics an anisotropic quality.

The use of honeycomb material has various disadvantages when it comes to impact damage. It is difficult to withstand highly localized external stresses and to determine how damage would affect the material. The quality and resistance of structures made with honeycomb are critically dependent on the resin used at the interface between core and skin. The strength of this adhesive greatly influences the strength of the panel. This is because the resistance sandwich structure against impact is directly related with the integrity of the components.

1.7 Cell Configurations

The hexagon, square, and flex-core are the three fundamental cell forms. The over-expanded, under-expanded, and reinforced configurations are a few variants of these designs. All of these setups are displayed in Figure 1.6.

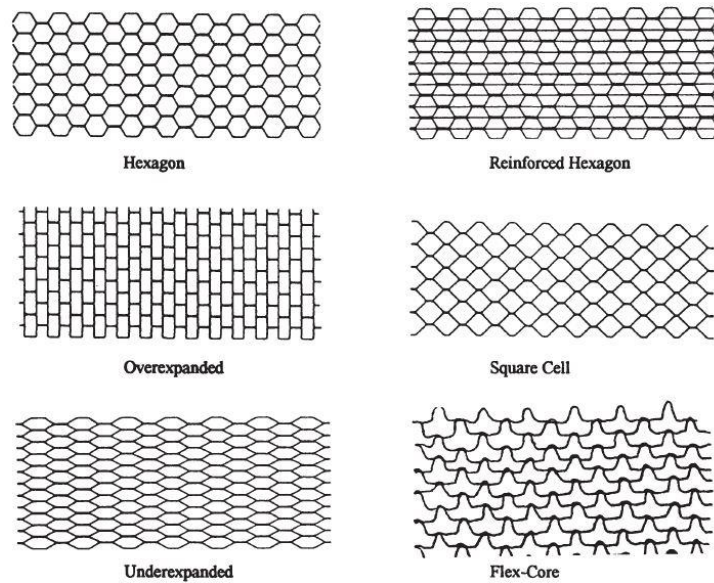


Fig. 1.6 Honeycomb cell configurations (Bitzer 1997)

The majority of resistance welded and brazed cores have square cells, whereas hexagonal cells (very narrow nodes) are the most common in adhesively bonded honeycomb. The conventional hexagon has simply been extended into a rectangle in the over-expanded core. When the honeycomb must be created using compound curves, Flex-Core is employed since this design may be wrapped around a tiny or spherical object. In order to improve the density of the reinforced honeycomb and its accompanying mechanical qualities, an additional flat sheet is positioned at the nodes.

1.8 Honeycomb Properties and Application

The following honeycomb mechanical characteristics are often assessed like shear strength and moduli of L & W plate, stabilized compressive strength and moduli. Approximately 50% of the bare compressive strength is required for crush strength in energy absorption applications. The following are some attributes:

1. Ratio of strength to weight is high.
2. Strength is high
3. Stiffness is high
4. Weighs light
5. High capacity to absorb specific energy.
6. Thermal protection.

The basic reason is to save weight. However, smooth skins and excellent fatigue resistance are also attributes of a honeycomb panel. The fatigue resistance of sandwich

Introduction... ✍

structure is still another significant benefit. The outcomes of acoustic fatigue experiments contrasting a honeycomb panel with a skin-stiffened structure are shown in figure 1.7. Keeping in mind that the conventional structure only lasted 3 minutes while the honeycomb panel lasted 460 hours at 167 dB. As a result, the honeycomb panel had a 9200-fold longer lifespan (**Bitzer 1997**).

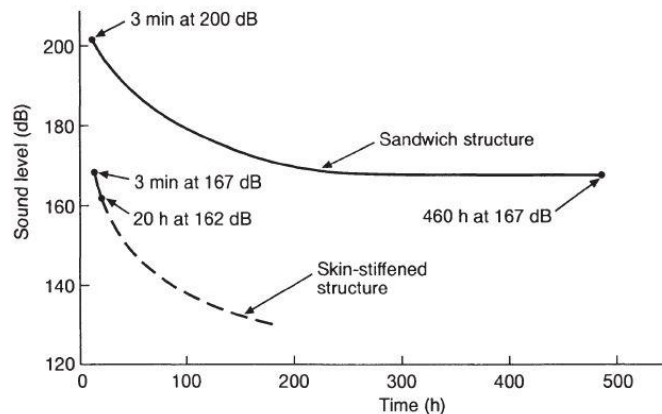


Fig 1.7 Comparative sonic fatigue resistance of conventional and sandwich structures (Bitzer 1997)

Weight reduction is yet another benefit of adopting honeycomb. It contrasts the stiffness and strength ratings of several honeycomb architectures. Despite being 7 times more bending-resistant and 37 times more rigid than a flat aluminium sheet, the sandwich weighs just 9% more than a solid plate. Where low-weight is a design consideration, honeycomb should be used if the structure buckles. (**Bitzer 1997**).

In addition to these mechanical features, honeycomb structures have several structural uses. Sandwich structures are becoming more and more significant. These are comparable to the fields of architecture, sports equipment, furniture manufacturing, aerospace and aviation, building projects, and car panels, among others.

1.9 Failure Modes of Honeycomb Structure

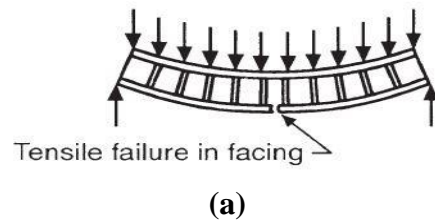
The four basic types of damage to a crushed honeycomb structure are layer breaking, core crushing, core tearing, and core splitting. The following are a few examples of the various situations for sandwich panel failure and their causes:

1. Facing failure
2. Transverse shear failure

3. Flexural crushing of core
4. Local crushing of core
5. General buckling
6. Shear crimping
7. Face wrinkling (core) and face wrinkling (adhesive)
8. Intracell buckling (dimpling)

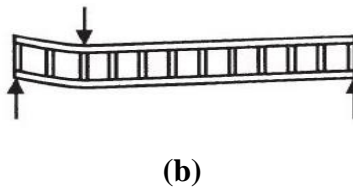
1.9.1 Facing failure

Due to insufficient panel thickness, facing thickness, or facing strength, the initial failure may happen on either the compression face or the tension face.



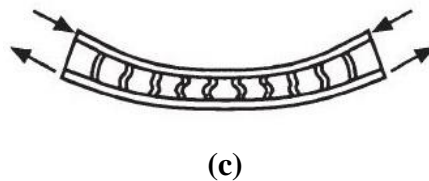
1.9.2 Transverse shear failure

Due to insufficient panel thickness or core shear strength.



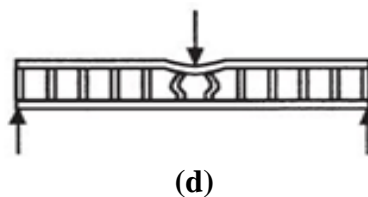
1.9.3 Flexural crushing of core

Due to excessive beam deflection or inadequate core flatwise compressive strength.



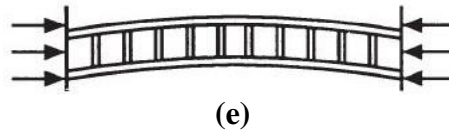
1.9.4 Local crushing of core

Due to weak core compression strength.



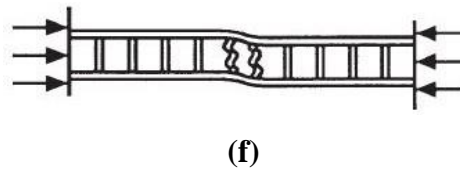
1.9.5 General buckling

Due to insufficient core shear stiffness or panel thickness.



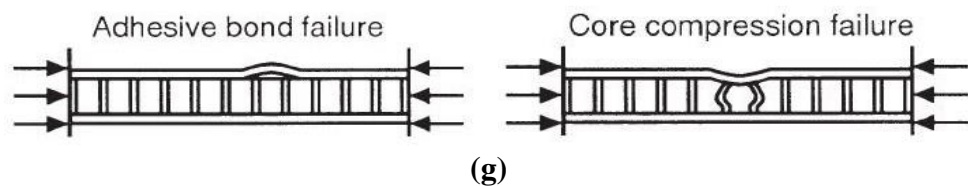
1.9.6 Shear crimping

Poor core shear modulus or low adhesive shear strength are the main causes of general buckling.



1.9.7 Face wrinkling

Depending on the relative strengths of the core in compression and adhesive in flatwise tension, it may buckle inward or outward.



1.9.8 Intracell buckling (dimpling)

Only applies to cellular cores. Large core cells and extremely thin facings cause this to happen. Failure might result from this action spreading to neighboring cells, which would result in wrinkles on the face.

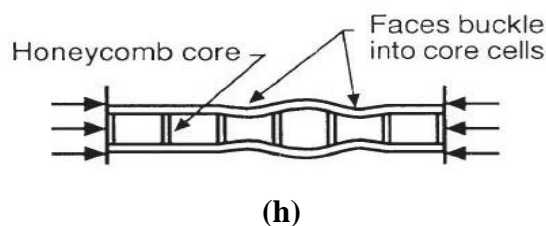


Fig.1.8 (a) Facing failure; (b) Transverse shear failure; (c) Flexural crushing of core; (d) Local crushing of core; (e) General buckling; (f) Shear crimping; (g) Face wrinkling (core) and face wrinkling (adhesive); (h) Intracell buckling (dimpling) (Bitzer 1997)

1.10 Hierarchical Honeycomb

A new generation of lightweight honeycomb structures has been created in response to the increasing need for lightweight materials. Hierarchical honeycombs can greatly enhance the material qualities over conventional honeycombs while reaching lower densities and greater stability. Research on hierarchical structures has been actively undertaken in the realm of lightweight design.

A hierarchical honeycomb structure is created by replacing the vertices of a standard hexagonal lattice with smaller hexagons or larger hexagons while simultaneously lowering the wall thickness to maintain a constant overall density. This concept of structural multipolarity was initially introduced in 1993, after the microstructure and macrostructure of human bone. By joining multiple tiny primary honeycomb structures, he was able to create secondary honeycomb structures. According to the test, the secondary structure's compressive strength was 3.2 to 3.4 times greater than that of the primary structure (**Lake 1993**).

Responses at different length scales and degrees of hierarchy affect the overall mechanical behaviour of these structures, and greater levels of structural hierarchy can result in lighter-weight and better load bearing structures.

1.11 Aim of Thesis

This thesis is based on the stiffness analysis of the honeycomb sandwich composite which is having the boundary condition of bending test. The specimen is loaded with the three-point bending setup and the static load is applied on mid of the span. Out-of-plane crushing force is applied in hierarchical honeycomb structure. Various combination like first order hierarchical super structure with optimized geometries are examined. Total deformation that are present after applying forces are determine with the help of finite element method using static structural element module in ANSYS Workbench-R1 2022.

1.12 Thesis Outline

For any comprehensive structural analysis, it is required to bring together all the failure theories and structural behaviour of the particular hierarchical geometry. In this regard, this thesis follows the same procedure. This thesis begins with historical to modern era aspects, before moving on to original new work and then showing the analysis aspect of the hierarchical honeycomb structure. Thesis chapters' description is as follows:

Chapter 1 provides a brief history of the evaluation of honeycomb structures, followed by a discussion on cellular solids and their divisions. The components of a honeycomb composite sandwich structure, followed by the manufacturing process of the honeycomb core, materials, cell configuration, etc. Then some honeycomb properties with application. After that, which are the criteria under which the failure of a honeycomb structure is considered to yield or fail. At last, there is the introduction of the hierarchical honeycomb structure, explaining its advantages over the conventional hexagonal honeycomb structure.

Chapter 2 covers a complete literature assessment of honeycomb structure geometry alterations such as cell length change, cell wall thickness change, cell height change, material changes, and so on. The addition of super-structure alters the mechanical characteristics of the honeycomb sandwich construction, which is also discussed in this article. A summary of the findings of several researchers working in the topic of honeycomb structure improvement is provided. In addition, the chapter discusses the research gap and the objectives that might be used to overcome it.

Chapter 3 contains a detailed methods and resources utilised in this investigation. This chapter provides a full explanation of the many theories and performance factors used in this numerical study. This chapter also includes a discussion of various boundary conditions as well as the modelling technique for a super-structure honeycomb sandwich structure in SolidWorks and the ANSYS Workbench-R1 version.

Chapter 4 contains the findings of a numerical study of the honeycomb sandwich construction. It also contains validated of (**Hussain *et al.* 2018**) experimental findings to compute the stiffness of a sandwich construction with numerical approach. This chapter also includes a numerical simulation to determine the deformation created in the structure once the superstructure is introduced into the base geometry. This chapter also discusses on mess convergence.

Chapter 5 summarizes the work done for this research, followed by the conclusion. This chapter also comprises of future work that can be conducted to improve structural properties.



Review
of
Literature



2.1 General

Natural honeycomb structures have served as an inspiration for the creation of low density, high stiffness structures with a variety of practical applications. Studies have revealed that the structure depends on the honey comb shell's shape, the thickness of the cell walls, the height of the cells, and the qualities of the materials. After careful observation, it has been discovered that some adjustments to these values can improve the stability of the honeycomb sandwich construction. The following examples of studies that support approach are provided.

2.2 Analysis of Geometry Change

Chawla *et al.* (2003) forecasted the behaviour of honeycomb structures by means of finite element approach. Using PAM-CRASHTM, an explicit analysis algorithm, a dynamic analysis of hexagonal aluminium honeycomb structures was performed. The results were validated against experimental data. It has been determined that the simulation settings and honeycomb crushing behaviour are related. The simulation findings are also contrasted with values that have been expected theoretically. It was observed that the crushing strength of a honeycomb structure is influenced by both its geometry and the material characteristics.

Hong *et al.* (2006) experimentally found that typical crush strengths are lower under compressive and shear stresses than they are under pure compressive pressures. A phenomenological yield criteria for specimens with varying in-plane orientation angles is offered based on the normal crush and shear strengths performed experimentally under combined loads. The in-plane orientation angle rises, which makes the non-normality flow behaviour more obvious. According to the experimental findings, the energy absorption rate is also influenced by the angle of in-plane orientation. As a result of the unequal placement of horizontal plastic hinge lines and the rupture of aluminium cell walls along the adhesive lines, specimens crushed under combined pressures also exhibit inclined stacking patterns of folds. Typical crush strengths are lower under compressive and shear stresses than they are under pure compressive pressures.

Aktay et al. (2008) examined by creating a number of numerical algorithms for simulating the transverse crushing behaviour of honeycomb core materials and comparing. Since the micromechanics model can be used to calculate crush energy absorption for various honeycomb cell sizes, cell wall thicknesses, and cell materials, it is demonstrated that the model is appropriate for honeycomb design. It is not suited for analysis of massive sandwich structures due to the need for very tiny meshes, though. The homogenized FE model may be used to such a structure, however it provides poor agreement when core crushing causes collapse. Since the discrete particles can accurately simulate the material compaction during crushing, the SAC model is demonstrated to be the best suitable for application in structural modelling with substantial compression core crush failures. Test results on honeycomb made of Nomex and aluminium. These models were utilised in conjunction with a semi-adaptive numerical coupling (SAC) methodology.

Rao et al. (2012) theoretically estimated the strengths of honeycomb sandwich panels constructed of various materials. Aluminium alloys, high tensile steels, titanium, or composites were employed as the materials for the face skins. Sandwiches may be made using a variety of basic materials and forms. Among these, it was discovered that the aluminium honeycomb core provided significant weight savings as well as low manufacturing costs. Under lateral crushing force, a crushing test was conducted on aluminium honeycomb sandwich panel specimens while altering the cell thickness and height of the honeycomb core. It was found that the honeycomb core's crushing behaviour is unaffected by the height of the core. However, a crucial factor impacting the crushing strength of sandwich panels due to lateral pressure loads is the honeycomb core cell's wall thickness.

Abadi et al (2015) experimentally studied that static behaviour does not appear to be adequate to characterize the honeycomb sandwich panels effectively. It is necessary to get more details regarding the qualities of fatigue data. Important experimental fatigue results for honeycomb sandwich panels with and without fabricated faults are presented in this paper. Comparisons are made between the honeycomb sandwich panel fatigue test results and the skin made of an aluminium alloy (the reference case). The results of the experiments demonstrated that imperfections have no impact on the material's static behaviour. Compared to the W-direction, the L arrangement has a longer lifespan. Brinell lifetime is less susceptible to flaws of the drilling hole type than sandwich panel lifetime.

Nazeer et al. (2015) investigated the thermal analysis of square and hexagonal honeycomb structures with the structural analysis of such structures. An engineer must ascertain details such structural loads, geometry, support, conditions, and material qualities in order to conduct an appropriate analysis. Structural study often yields displacements, stresses, and deformations. Then, this data is contrasted with standards that denote failure circumstances. Temperature distribution and associated thermal quantities are computed during thermal analysis. The temperature distribution, the duration to study state, the study state temperature distribution (using a transient analysis), are to be analyzed. The temperature distribution after 50 seconds, the quantity of heat lost or gained, thermal gradients, and thermal fluxes are typical thermal attributes of importance.

Joshilkar et al. (2018) analyzed that the most highly regarded structural engineering advancements made in the composites sector is the honey comb sandwich architecture. It has uses in the rail, aerospace, aviation, and transportation sectors, among others. The behaviour of honeycombs subjected to three-point bending is investigated using Hypermesh and LS-DYNA. To validate the finite element (FE) findings for deflection and critical load, theoretical computations are employed. In CA114 software, a CAD model of the honey-comb sandwich is created. Copper, steel, aluminium, and titanium are the main materials utilised in the analysis, while steel is the material used for faceplates. The analysis is done by altering the honey comb's core wall and faceplate thickness. Graphs were created using the FEA findings that were received.

Upreti et al. (2020) analyzed current work uses FE-based software ANSYS to examine the natural frequency of a honeycomb sandwich composite construction made up of a Al 5052 hexagonal honeycomb core material and a carbon/glass fibre unidirectional facing sheet. Under static loads, natural frequencies were computed for specimens with face sheet thicknesses ranging from 0.5 mm to 2.5 mm. With an increase in face sheet thickness, it was discovered that the natural frequency rose and converged. With a rise in face sheet thickness, deformation and equivalent Von Mises stresses were expected, and they were observed to decrease.

Ugur et al. (2020) experimentally and numerically evaluated the behaviour of aluminium honeycomb structures under low-speed impact. Aluminium honeycomb composite structures were created utilizing a variety of adhesives with varying widths and

heights. The ASTM D7766 standard was followed when the generated honeycomb structures underwent low-velocity impact tests. The force values that produced damage to the structure were measured over time as a consequence of the experiment, and the highest force values were recorded. According to study, when cell width, height, and the quantity of multiwall carbon nanotubes drop, the maximum impact force values observed in honeycomb composite structures increase. It is seen that the results obtained by the finite element method and the experimental results are approximately 85% in agreement. There was no statistically significant difference between the results as a result of conducted t-test.

Ali et al. (2021) examined the distribution of stress and strain in sandwich constructions made of hexagonal aluminium cores and glass fiber face sheets. The aluminium honeycomb sandwich panels with face sheets function as a protective device to stop the failure of a significant structure that is under stress. It is crucial to do a research on the distribution of stress and strain on aluminium honeycomb with face sheets. Using Pro-E software, a model of hexagonal aluminium sandwich panels with glass fiber face sheets will be created. Further, ANSYS software will be used to analyses the stress and strain distribution for glass fiber face sheets with aluminium honeycomb. The hexagonal aluminium honeycomb face sheets with thicknesses of 0.5 mm, 1 mm, and 1.5 mm were subjected to an ANSYS study, which should be effective for a variety of applications.

Ghongade et al. (2021) analyzed the impact of reinforcement on the axially compressed circular core honeycomb construction. Using Abaqus-CAE, the load bearing capacity numerical analysis is carried out. Steel honeycomb panels (with and without reinforcements) are made using furnace-brazing technique in a continuous furnace for experimental validation. Despite the reinforcements adding weight to the panel, a significant increase in load bearing ability (44 percent) is seen. According to the findings, a reinforced honeycomb construction with cells that are 10 mm in diameter offers the best load bearing capability. The generated numerical model is supported by the experimental findings. According to the test findings, the reinforced honeycomb construction (10 mm in diameter) had a 20% greater density and 44.6% lower stresses than the traditional honeycomb structures.

Lubis et al. (2021) investigated the energy absorption using aluminium honeycomb structures with different sized hexagons. Three samples with different hexagonal diameters were used to assess this test. Each specimen's voltage data, strain, and energy suppression have been examined to determine which was more successful. The ability to absorb energy and strain in both horizontal and vertical testing orientations was demonstrated by a voltage graph of the test. It was found that object's capacity to absorb energy is directly correlated with its cross-sectional area. The specimen's shear voltage strength is significantly influenced by the stiffness of the glue or matrix on the core. Horizontal testing position with a hexagonal size of 2 mm yields the highest energy absorption results, while the vertical testing position with a hexagonal size of 6 mm yields the lowest.

Ciepielewski et al. (2022) analyzed the static and dynamic compressive loads examination of certain aluminium honeycomb sandwich materials. Static strength machine, drop hammer, and Split Hopkinson Pressure Bar are some of the employed equipment (SHPB). The outcomes demonstrate how applied strain rate affects the tested material's strength characteristics, particularly Plateau stress. With an increase in the strain rate of, on average, 10% to 19%, it was seen in each of the situations addressed that the value of plateau stresses increased across the board. Given the geometrical characteristics of the samples, the plateau stress increase between samples with the smallest and largest cell sizes for the SHPB test was approximately 0.3 MPa and approximately 0.15 MPa for the drop hammer test, respectively. This increase is primarily noticeable in the final phase of structure destruction.

Kaveloglu et al. (2022) experimentally focused on the maximal compressive force of honeycomb structures created using an Ultimaker hot plate 3D printer. Filament used in the experiment was made of polylactic acid (PLA) and acrylonitrile butadiene styrene. The samples were made with three different cell widths: 6 mm, 9 mm, and 12 mm; three different cell wall thicknesses: 0.8 mm, 1.2 mm, and 1.6 mm; and three different cell heights: 10 mm, 20 mm, and 30 mm. Weighing the generated samples enabled to evaluate porosity percentages of 3D printed core. In the compression test, samples made from PLA filament with cell dimensions of 10 mm in height, 12 mm in width, and 1.6 mm in wall thickness yielded the maximum compressive forces. Similar findings were obtained using

ANSYS software. When compared with experimental setup, it was found that results from ANSYS have an accuracy range of 81 to 98%. Thus, it was shown that the wall thickness was directly linked to a larger maximum compressive force.

Onyibo and Safaei (2022) analyzed the finite element analysis software's design of honeycomb sandwich constructions. The characteristics of honeycomb at the microstructure and unit cell levels is determined. Because the experimental technique may be time and money-consuming, there is now capacity for extensive FEA study on loading response with different cores and thickness in order to examine the mechanical characteristics. This study concentrates on the FEA of honeycomb sandwiches that have been performed by several studies using the commercial software programmers ANSYS and ABAQUS. It will serve as a reference for future studies to examine what has been accomplished and what may be achieved using FEA software. Numerous studies' descriptions of the experiment's specifics are by no means clear yet information on things like web thickness, ply angle, sandwich weight, resin type, area/volume of the honeycomb structure, and sandwich cell count is sometimes left out entirely. The carbon fiber composite curved honeycombs (CCCHs) are the best honeycomb load-bearing components.

2.3 Analysis of Hierarchical Structure

Taylor *et al.* (2011) studied the elastic and structural characteristics of hierarchy honeycomb. Using finite element modelling, the effects of adding hierarchy to a variety of honeycombs with triangular, square and hexagonal shaped super and sub-structure cells were investigated. The relative lengths and mass shared by the sub-structures and super-structures were key characteristics determining these geometries. The incorporation of a hierarchical substructure into a honeycomb reduces the in-plane density specific elastic modulus. When compared to a regular non-hierarchical form, there is often a 40 to 50% decrease. More complicated substructures, such as graded density, can recover density specific elastic modulus values. It was feasible to exceed the density specific modulus of traditional versions by up to 75% with careful design of functionally graded unit cells. A negative Poisson's ratio substructure also resulted in significant increases in density modulus when compared to ordinary honeycombs.

Chen and Pugno (2012) investigated the elastic buckling of a novel type of honeycomb materials with hierarchical architecture. The virtual buckling stresses and related strains for each cell wall at the $n-1^{\text{th}}$ level are estimated from n^{th} using the top-down technique. The true local buckling stress was then calculated by comparing the virtual buckling stresses of all cell walls. The hierarchical structure's gradual collapse was investigated. Finally, parametric analysis identified several important factors influencing local buckling stress and strength-to-density ratio. As the hierarchy n^{th} level increased, the constitutive behaviour and energy-absorption characteristics were computed. The results demonstrated that the elastic buckling characteristics could be tailored at each hierarchical level and may be utilised to develop multiscale energy-absorption honeycomb light materials.

Mousanezhad *et al.* (2015) experimentally and numerically investigated the fresh insights into the behaviour of structurally hierarchical auxetic metamaterials. It was shown that introducing hierarchy-dependent elastic buckling at relatively early stages. The deformation reduces value of Poisson's ratio as the structure is squeezed uniaxially, resulting in auxeticity in later stages of deformation. This unusual behaviour, which is caused by structural hierarchy, has not been detected in the non-hierarchical normal structure. When squeezed in the same direction, the suggested hierarchical design demonstrated two distinct deformation modes for structures with varied geometrical features. The structures with the first order of hierarchy reached an ideal design in terms of the lowest Poisson's ratio, which coincides with a point when the buckling modes interchanges. By introducing higher tiers of hierarchy, the auxetic response can be enhanced (i.e., lower Poisson's ratio).

Ghaedizadeh *et al.* (2016) experimentally and numerically simulated validation of present study. Here, a square lattice was converted into a 2D auxetic metamaterial. By altering the initial form of the microstructure with the appropriate buckling pattern, the metallic metamaterials subsequently exhibit auxetic behaviour with controllable mechanical properties. A thorough parametric investigation using tested finite element models was done to uncover the novel properties of metallic auxetic metamaterials undergoing considerable plastic deformation. The research findings were a helpful guide for developing 2D metallic auxetic metamaterials for a number of applications. It was

discovered that the stiffness and strength of metallic metamaterials may be changed separately by adjusting the base material's characteristics while the negative Poisson's ratio remains essentially constant.

Ingrole *et al.* (2017) analyzed a new auxetic-strut structures with improved performance were designed in a unique way. Using 3D printing, researchers compared the in-plane uniaxial compression loading behaviour of conventional honeycomb, locally reinforced auxetic-strut structure, re-entrant auxetic honeycomb, and a hybrid construction combining conventional honeycomb and auxetic-strut structure. Auxetic honeycombs with a negative Poisson's ratio have recently become the subject of investigation (NPR). The unique mechanical characteristics, volume change control, and superior impact energy absorption performance of auxetic structures make them appealing for a variety of technical applications. Different cells' deformation and failure mechanisms were investigated, and their functionality was also covered. The novel auxetic-strut structure outperformed the honeycomb and auxetic structures in terms of mechanical qualities. The new design can absorb more energy than the previous buildings since it has lower Poisson's ratio values.

Qin *et al.* (2020) investigated failure modes and energy absorption processes of Out-of-plane dynamic crushing with metal hierarchical honeycomb structures having porous walls. The impact failure modes were obtained at various impact velocities. The associated numerical simulations were also carried out. It showed that the numerical results match well with the experimental data. The dynamic mean crushing stress of hierarchical honeycomb structures was larger than their quasi-static mean crushing stress. The mean crushing stress, total energy absorption and specific energy absorption of pores on double walls are greater than those of perforations on single walls of the same mass. The findings of a parametric investigation of parameters influencing the dynamic crushing response of hierarchical honeycomb structures were reported. The perforation gradient designs enhance the mean crushing stress as compared to the uniform perforation design.

Chandrashekhar *et al.* (2021) analyzed the behaviour of a hybrid honeycomb structure over solid-profile structures. A common use of honeycomb structure is in sandwich panels, which have a high stiffness-to-weight ratio, a low mass-to-volume ratio, and a high energy absorption capacity. The different hybrid hollow structures with finite boundaries

(finite length and width) and a compressive load are studied using the finite element technique. Static structure simulation is used to process these structures' stress and deformation characteristics and produce the necessary data. In this study, a comparison of many hybrid structures is done based on the data acquired to assess how adaptable they are.

Dhari *et al.* (2021) investigated the deformation processes of re-entrant honeycomb auxetic structures under inclined loads. During a static study, an auxetic nite-element prototype was squeezed by a stiff plate. Analyzing the structure's deformation response indicated the creation of a new transitional deformation stage that severely limits the elastic response. This new macro stage is made up of a series of plateau-densification (yielding-hardening) micro stages that correlate to a highly localized deformation mode and modify the mechanical response in the subsequent macro stages. The study demonstrated that tilted loads trigger a novel response mechanism in RHS auxetic structures. Under dynamic loads, which are frequently stochastic, such a resistant system becomes very fascinating. As self-contact occurs inside, a more compliant reaction with increased dampening might be predicted.

Peng *et al.* (2021) investigated hybrid-honeycomb structure with increased rigidity. It is made up of two merged hexagonal honeycombs. The effective thermoelastic characteristics were evaluated using analytical and computational homogenization approaches. The effective Young's modulus, Poisson's ratio, and thermal expansion coefficient were all expressed analytically. The structure's effective thermoelastic characteristics were broadly modifiable by modifying the microstructural geometry and component materials. The in-plane efficient Poisson's ratio and thermal expansion coefficient were modified from negative to positive throughout a wide range. The structure might also be built to have improved stiffness, a high degree of auxeticity, and negative thermal expansion by carefully selecting the geometrical and material characteristics.

Jiang *et al.* (2022) investigated about enhancing the material's strength and energy absorption capabilities, the double circular arc walls were added into the normal DAH unit cell. Upper-circular (U-type), lower-circular (L-type), and full-circular circular double arrowed honeycomb (CDAH) unit layouts were presented (F-type). DAH and CDAH prototype specimens were created via 3D printing and evaluated under quasi-static crushing. The experimental data were used to develop and validate the specimen finite

element (FE) models. According to experimental and computational data, the three kinds of circular double arrowed honeycomb (CDAH) exhibit higher compressive stress, crush force efficiency (CFE), and specific energy absorption (SEA) than the DAH with the same geometric properties. Finally, by logically constructing the arc wall location and the geometric parameters of the unit cell, a broad range of SEA and Poisson's ratio of the CDAH can be produced.

Zhong *et al.* (2022) investigated that due to distinct deformation characteristics, auxetic materials show favorable mechanical qualities, such as fracture resistance, shear resistance, and energy dissipation. Sandwich constructions made of honeycomb also offer outstanding qualities, such as low density and effective energy absorption. These positive traits make them promising alternatives for building construction that can satisfy the demands of modern construction, which call for a higher safety standard. Through a quasi-static compression test, the performance of the multilayer honeycomb sandwich structure's energy absorption was assessed. According to the findings, the layered structure has a larger initial peak stress and a more stable platform stress. Additionally, it could increase the structure's overall stability and shear resistance. These results are helpful for auxetic metamaterial applications in building construction.

Wannarong *et al.* (2022) examined the mechanical properties of Acrylonitrile Butadiene Styrene (ABS) and Polylactic Acid (PLA) generated using additive manufacturing. ABS and PLA are the most often used materials for cores. The behaviour of cores was also investigated. The re-entrant core, which showed negative Poisson's ratio or auxetic behaviour, was identified to increase bending stiffness. Sandwich structure bending and fatigue performance was influenced by core densities, core designs, component materials, face sheet thickness, and face sheet stacking sequence. Furthermore, the results showed that finite element analysis may be used to analyze the mechanical properties of sandwich structures with honeycomb cores. It has been demonstrated that the bending performance and fatigue behaviour of a sandwich may be estimated using finite element analysis.

2.4 Research Gaps

It has been observed from above literature summary that adding a sub-structure to a conventional honeycomb structure improves the material's mechanical characteristics

compared to the basic one. No work has been submitted where super-structure are introduced into hexagonal honeycomb sandwich structure. Combined effect of both sub-structure and super-structure is yet to be analyzed. Work is yet to be done on face Sheet of honeycomb sandwich structure which are made up of composite materials. It should be remembered that the honeycomb construction's faceplate and core wall thickness both increase the core's capacity to support loads.

2.5 Objectives

The geometry of the honeycomb cell width, cell thickness, cell height, angle of orientation etc. plays a crucial part in creating a better core. A thicker face sheet increases the structure's ability to absorb energy, while a better bonding glue makes the structure more stable. The following are the main objectives of the current work:

1. Validation of experimentally performed static bending with finite element analysis.
2. Mesh convergence analysis is used to choose an appropriate mesh size for simulating out-of-plane static bending.
3. Adding super-structure into the base geometry of hexagonal honeycomb core.
4. Changing geometric parameters of super-structure like cell length, cell height, cell wall thickness etc.



Materials
and
Methods



Chapter 3

MATERIALS AND METHODS

3.1 General

This chapter describes the methods and process for conducting a static analysis on a honeycomb sandwich construction. A sub-structure of hexagonal cells is added to each node of a typical honeycomb to create a hierarchical honeycomb. The three point bend specimen is used in static analysis to determine the sandwich structure's stiffness. Deformation is calculated through FEM for every geometric change.

3.2 Density of hexagonal cell

Any cellular structure's relative density is a key factor in determining its mechanical characteristics. Relative density is the ratio of a substance's density to the density of a certain reference material. Relative density is defined as follows-

$$\text{Relative density} \left(\frac{\rho^*}{\rho_s} \right) = \frac{\text{Density of cellular material } (\rho^*)}{\text{Density of solid from which the cell walls are made } (\rho_s)} \quad (3.1)$$

Consider the length l and thickness t of a regular hexagonal honeycomb. When effective thickness is taken into account, the effective length of one unit cell is $t/2$, with material density ρ_s and breadth b as shown in Fig. 3.1.

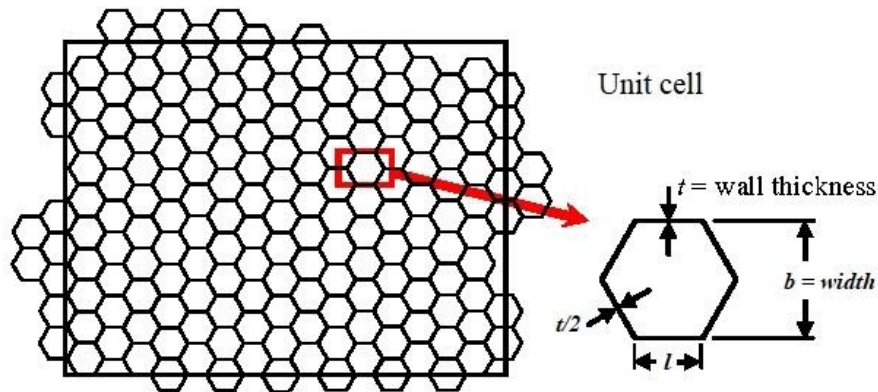


Fig. 3.1 Hexagonal honeycomb unit cell

The length of inner side wall will be defined as:

$$l^* = l - 2 \left(\frac{t}{2} \right) \frac{1}{\tan \frac{\pi}{3}} = l - \left(\frac{t}{\sqrt{3}} \right) \quad (3.2)$$

Density of honeycomb unit cell ρ^* = (mass/volume)

$$\text{Mass of unit cell} = 6 \left[\frac{\sqrt{3}}{4} l^2 - \frac{\sqrt{3}}{4} \left(l - \frac{t}{\sqrt{3}} \right)^2 \right] \times b \times \rho_s \quad (3.3)$$

$$\text{Volume of unit cell} = 6 \left(\frac{\sqrt{3}}{4} l^2 \right) b \quad (3.4)$$

$$\text{Density of unit cell, } \rho^* = \frac{6 \left[\frac{\sqrt{3}}{4} l^2 - \frac{\sqrt{3}}{4} \left(l - \frac{t}{\sqrt{3}} \right)^2 \right] \times b \times \rho_s}{6 \left(\frac{\sqrt{3}}{4} l^2 \right) b} \quad (3.5)$$

$$\text{Actual relative density, } \frac{\rho^*}{\rho_s} = \frac{2}{\sqrt{3}} \left(\frac{t}{l} \right) - \frac{1}{3} \left(\frac{t}{l} \right)^2 \quad (3.6)$$

Considering cell wall thickness t very small so neglecting higher power terms we get-

$$\text{Relative density, } \frac{\rho^*}{\rho_s} = \frac{2}{\sqrt{3}} \left(\frac{t}{l} \right) \quad (3.7)$$

3.3 Deformation mechanism in honeycomb core

When we consider the deformation mechanism of the honeycomb core, we can observe that in-plane deformation impacts the core more than out-of-plane deformation. This is due to the bending of cell wall. But when we consider out-of-plane deformation, stiffness and strength are substantially higher because they require axial elongation or compression of the cell walls. Figure 3.2 depicts the honeycomb showing X_1 , X_2 and X_3 plains.

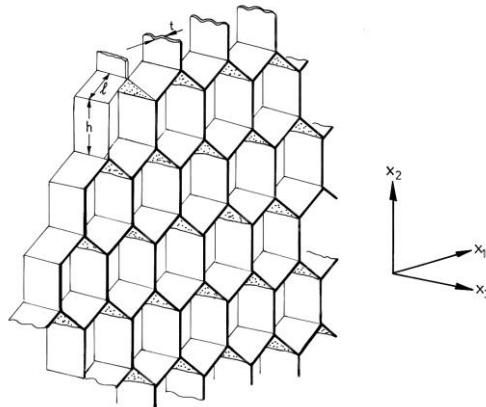


Fig. 3.2 Hexagonal honeycomb core with in-plane loading on plane X_1 - X_2 and out-of-plane loading on plane normal to X_3 (Gibson and Ashby 1997).

The out-of-plane analysis provides the extra stiffness required for the design of a honeycomb core in sandwich panels as well as a comprehensive description of the behaviour of natural honeycomb materials such as wood.

3.3.1 In-plane deformation

The cell walls deform under compressive pressure, resulting in linear elasticity (provided that the cell wall material is linear-elastic). When a certain stress level is reached, however, the cells begin to disintegrate. Collapse in elastomeric materials is caused by the elastic buckling of the cell walls and is hence recoverable. It is formed by the production of plastic hinges at the section of greatest moment in bent members in materials with a plastic yield point. Brittle fracturing of the cell walls occurs in brittle materials. At high stresses, the cells eventually collapse to the point where opposing cell walls meet (or their fractured pieces pack together) and additional deformation compresses the cell wall material. This results in the final, steeply increasing part of the stress-strain curve which is labelled densification. In-plane deformation can be visualized in Fig. 3.3.

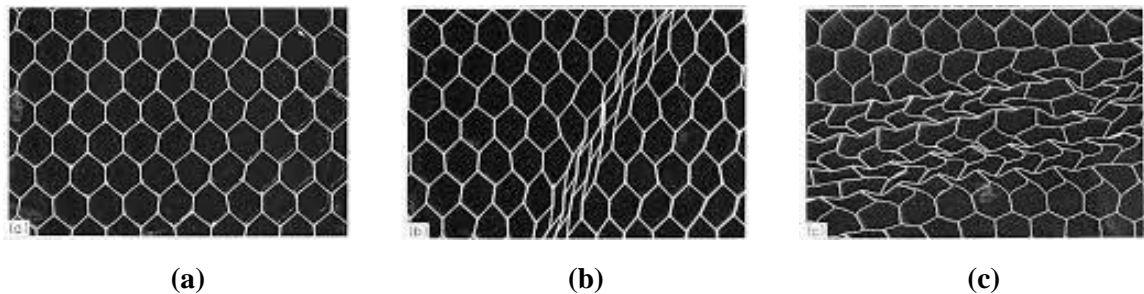


Fig. 3.3 In-plane deformation of honeycomb (a) an un-deformed honeycomb; (b) yielding of cell walls in X_1 direction (compression); (c) yielding of cell walls in X_2 direction (compression) (Gibson and Ashby 1997)

The relative thickness of the cell wall grows as the relative density of a honeycomb increases. When resistance to cell wall bending increases, cell collapse also increases. This results in greater modulus and plateau stress. Immediately following cell wall contact, reducing strain curve changes with densification.

3.3.2 Out-of-plane deformation

When loaded along the cell axis, honeycombs become significantly stiffer and stronger (X_3 direction). The same is true for honeycombs that have been loaded with out-of-plane shear (as they are in sandwich panels loaded with bending). The first linear-elastic deformation in these circumstances involves considerable axial or shear deformations of the cell walls themselves. The linear-elastic domain is shortened in compression by buckling (elastic for an elastomer, plastic for a metal or hard polymer) and

final failure occurs by ripping or crushing. The honeycomb is elastic in strain until it splits, gives plastically or fractures.

3.4 Properties of honeycomb cell

A hexagonal honeycomb unit cell is depicted in Fig 3.4 below. The load response in the X_1 - X_2 plane is investigated. The in-plane characteristics are isotropic if the hexagon is regular (sides are equal and angles are all 120°) and the cell walls have the same thickness. They are not affected by direction. A structure of this type includes two independent elastic moduli (a Young's modulus E and a shear modulus G) and a single plateau stress σ .

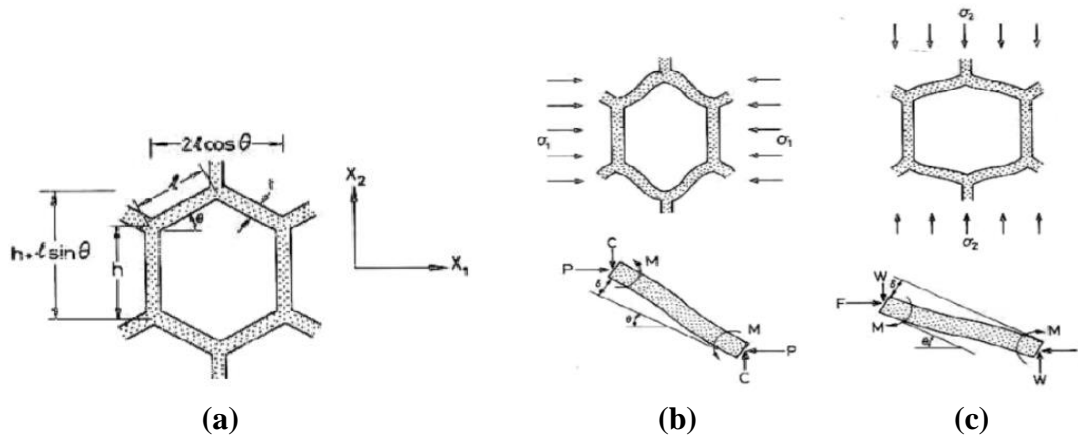


Fig. 3.4 Cell deformation due to elastic compression: (a) un-deformed honeycomb; (b) & (c) bending caused by loads in X_1 and X_2 directions (Gibson and Ashby 1997)

However, the characteristics are anisotropic when the hexagon is irregular (i.e. the cell walls in one direction are thicker than those in the other). The in-plane characteristics need four moduli (E_1^* , E_2^* , G_{12}^* and ν_{12}^* ; where ν_{21}^* is a Poisson's ratio) and two plateau stress values (σ_1^* and σ_2^*).

Here, we assume that honeycomb has a low relative density, $\frac{\rho^*}{\rho_s}$ therefore l/t is small. Relation between two is-

$$\frac{\rho^*}{\rho_s} = \frac{\frac{t}{l}(\frac{h}{l}+2)}{2 \cos \theta (\frac{h}{l} + \sin \theta)} \quad (3.8)$$

which is reduced to:

$$\frac{\rho^*}{\rho_s} = \frac{2}{\sqrt{3}} \frac{t}{l} \quad (3.9)$$

3.4.1 In-plane properties

When we study the in-plane characteristics of a regular hexagon honeycomb cell when the deforming force is applied, we see linear buckling in the honeycomb structure's cell walls. We can identify this buckling phenomena of cells using various equations. Modelling of in-plane loading behaviour is shown in Fig. 3.5.

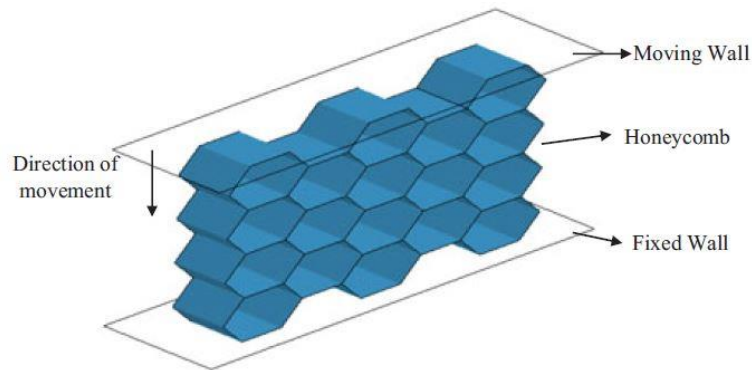


Fig. 3.5 In-plane loading of honeycomb core

The in-plane loading arrangement is shown above. Some in-plane properties are as follows:

1. Linear elastic deformation

The cell wall of a honeycomb bends in a linear-elastic way when loaded in the X_1 or X_2 directions is depicted in Fig. 3.6. Conventionally, the reaction is described as below:

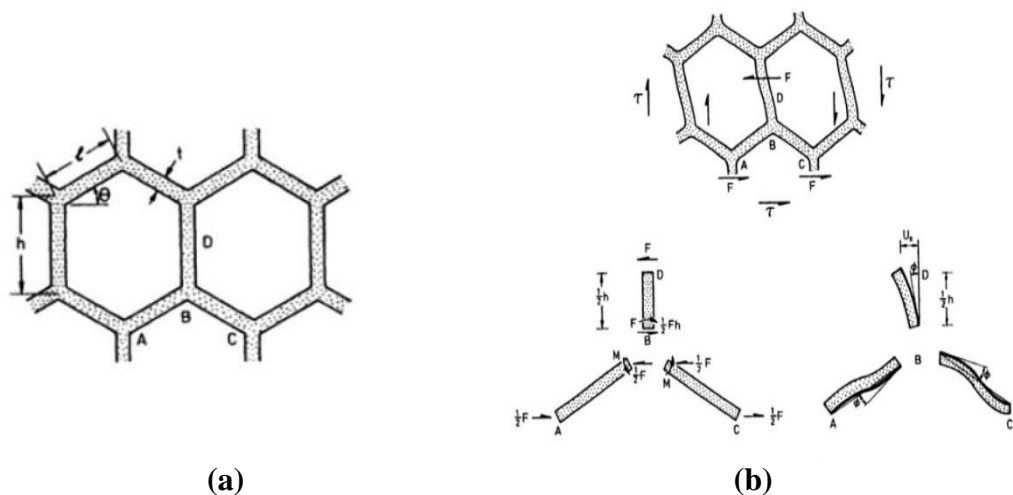


Fig. 3.6 Cell wall bending and rotation due to linear elastic shear: (a) un-deformed honeycomb (b) displacement and rotation due to shear stress (Gibson and Ashby 1997)

Due to this response at honeycomb core is described by five moduli i.e. two Young's moduli E_1^* , E_2^* , a shear moduli G_{12}^* and two Poisson's ratios ν_{12}^* and ν_{21}^* .

Young's modulus parallel to X_1 is just $E_1^* = \sigma_1/\epsilon_1$, given as

$$\frac{E_1^*}{E_s} = \left(\frac{t}{l}\right)^3 \frac{\cos \theta}{\left(\frac{h}{l} + \sin \theta\right) \sin^2 \theta} \quad (3.10)$$

Young's modulus parallel to X_2 is just $E_2^* = \sigma_2/\epsilon_2$, given as

$$\frac{E_2^*}{E_s} = \left(\frac{t}{l}\right)^3 \frac{\left(\frac{h}{l} + \sin \theta\right)}{\cos^3 \theta} \quad (3.11)$$

Shear modulus $G_{12}^* = \tau/\gamma$, given as

$$\frac{G_{12}^*}{E_s} = \left(\frac{t}{l}\right)^3 \frac{\left(\frac{h}{l} + \sin \theta\right)}{\left(\frac{h}{l}\right)^2 (1 + 2h/l) \cos \theta} \quad (3.12)$$

where τ is remote stress and γ is shear strain.

Poisson's ratio in X_1 and X_2 direction respectively, given as

$$\nu_{12}^* = -\frac{\epsilon_2}{\epsilon_1} = \frac{\cos^2 \theta}{\left(\frac{h}{l} + \sin \theta\right) \sin \theta} \quad (3.13)$$

$$\nu_{21}^* = -\frac{\epsilon_1}{\epsilon_2} = \frac{\left(\frac{h}{l} + \sin \theta\right) \sin \theta}{\cos^2 \theta} \quad (3.14)$$

3.4.2 Out-of-plane properties

The normal and shear loads are carried by the honeycomb cores in the surfaces perpendicular to the axis of the regular hexagonal honeycomb prisms. Honeycombs are very effective in this out-of-plane orientation. Modelling of in-plane loading behaviour is shown in Fig. 3.5

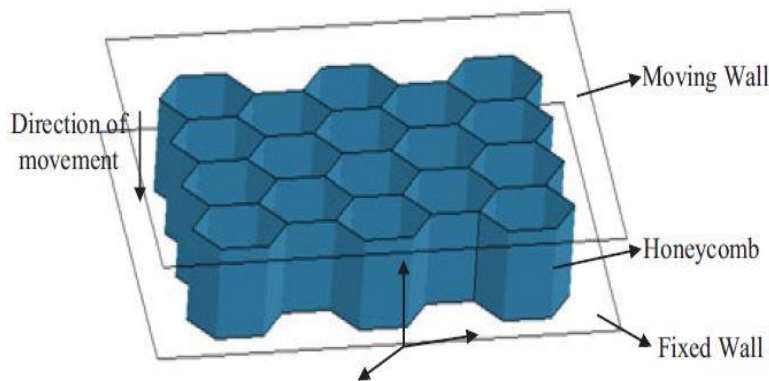


Fig. 3.7 Out-of-plane loading of honeycomb core

The in-plane loading arrangement is shown above. Some in-plane properties are as follows:

1. Linear elastic deformation

When a honeycomb is loaded in out-of-plane, the cell walls are expanded or compressed (rather than bent). Hexagonal honeycomb moduli are considerably larger than those computed for in-plane loading. The honeycomb core's role is to carry normal and shear stresses in planes including the axis of the hexagonal prisms, as seen in Fig. 3.8 below.

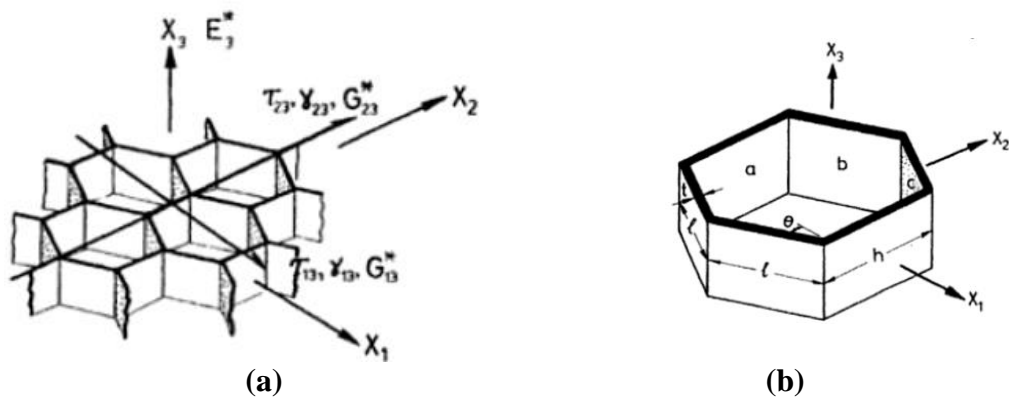


Fig. 3. 8 (a) honeycomb carrying loads on the faces normal to X_3 ; (b) one cell showing walls a, b, c (Gibson and Ashby 1997).

In the X_3 direction, Young's modulus E_3^* simply reflects a solid modulus E_s , scale by load-bearing section, given as

$$\frac{E_3^*}{E_s} = \left\{ \frac{\frac{h}{l} + 2}{2\left(\frac{h}{l} + \sin\theta\right) \cos\theta} \right\} \frac{t}{l} = \frac{\rho^*}{\rho_s} \approx \frac{t}{l} \quad (3.15)$$

Two more Poisson's ratios, ν_{31}^* and ν_{32}^* , are identical to those for the solid, given as

$$\nu_{31}^* = \nu_{32}^* = \nu_s \quad (3.16)$$

For X_1 direction shear modulus is evaluating, given as

$$\frac{G_{13}^*}{G_s} \leq \frac{\cos\theta}{\frac{h}{l} + \sin\theta} \left(\frac{t}{l} \right) \quad (3.17)$$

For X_2 direction shear modulus is evaluating, given as

$$\frac{G_{23}^*}{G_s} \leq \frac{1}{2} \frac{\frac{h}{l} + 2 \sin^2\theta}{\left(\frac{h}{l} + \sin\theta\right) \cos\theta} \left(\frac{t}{l} \right) \quad (3.18)$$

3.5 Bending energy due to crushing

Bending energy is the energy required to bend the wall. This is computed by multiplying the plastic bending moment by the angle at which the wall is bending. By adding the energy lost at three plastic stable hinge lines, the bending energy of every fold may be computed.

$$U_b = \sum_{i=1}^3 M_o \theta_i L_c \quad (3.19)$$

Where, M_o = plastic bending moment per unit width;

θ_i = hinged lines rotation

L_c = total flange length

σ_o = flow stress = $\sqrt{\frac{\sigma_y \times \sigma_u}{1+n}}$, σ_y = yield stress, σ_u = ultimate stress

The centre hinge line will have $\theta = \pi$ for full folding, while the top and bottom hinge lines will have $\theta = \frac{\pi}{2}$ with each bonding energy.

$$U_b = M_o(\theta_1 + \theta_2 + \theta_3)L_c \quad (3.20)$$

$$U_b = 2 \pi M_o L_c \quad (3.21)$$

3.6 Sub-structure (α) and super-structure factor (β)

FEM is used to investigate deformation and stresses in this work. A hexagonal substructure is introduced for each node in this case. When we talk about superstructure, we insert a bigger hexagon based on the centre of a standard hexagonal cell. So, in order to calculate the length of a side of a regular hexagonal sub-structure & super-structure, a factor ' α ' (for sub-structure) & ' β ' (for super-structure) is assigned as shown in fig 3.9. This factor is required for comparing different hierarchical geometries and for length calculation and comparison.

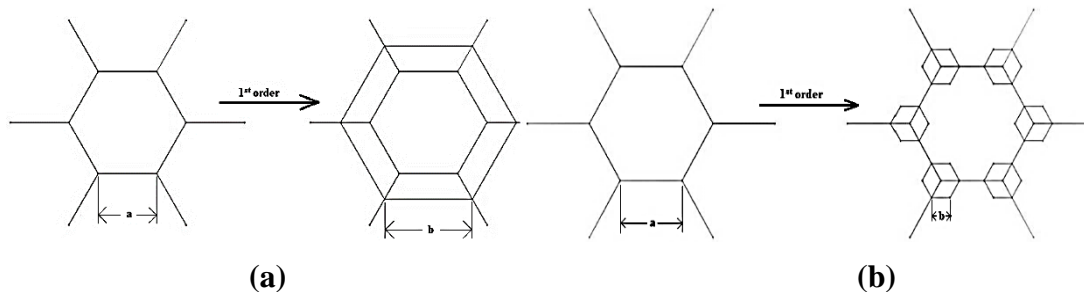


Fig. 3.9 (a) Unit cell with 1st order sub-structure hierarchy; (b) Unit cell with 1st order super-structure hierarchy

The minimal value of ' α ' for first order hierarchical sub-structure is 0 and the highest value is 0.5. The boundary requirement for the substructure's edge length is $0 \leq b \leq a/2$.

$$\alpha = \frac{\text{edge length of sub-structure } (b)}{\text{edge length of base structure } (a)} \quad (3.22)$$

While, the minimal value of ' α ' for first order hierarchical super-structure is 'a' and the highest value is 1.5. The boundary requirement for the super-structure's edge length is $a \leq b \leq 1.5a$.

$$\beta = \frac{\text{edge length of super-structure } (b)}{\text{edge length of base structure } (a)} \quad (3.23)$$

3.7 Modelling and FEM of sub-structure and super-structure using ANSYS

To determine the stiffness qualities of any element, analytical approaches, experiment methods, and numerical methods can be utilised. In ANSYS Workbench, a module called as Static Structure is used to solve the sandwich structure deformation and various stresses created in beam components.

Many engineering firms that deal with structures are now using Finite Element Methods to replace destructive testing of any component (FEM). The tested model is represented in modelling software throughout this procedure, and then the analysis is carried out. Although this technique is time-consuming and needs specialized knowledge, the specimen cost can be decreased.

In the current investigation ANSYS Workbench is used for FEM analysis, and the processes below are involved.

3.7.1 Structural modelling

Geometric modelling is carried out using the SOLIDWORKS modelling programme. To begin, a 2D sketch is created by selecting the top plane of the sketching tool. Then 2D sketch of a regular hexagon honeycomb cell of 3.4 mm side length and 0.25 mm cell wall thickness is created. A 2d honeycomb core with dimensions of 26x200 is drawn using a linear pattern. The honeycomb core drawing is then extruded to a height of 13.5 mm. Then, two face sheets with dimensions of 28x200 are drawn and extruded to 0.25 mm. When all three sections have been modelled, assembly may begin to make a full honeycomb sandwich panel. When the modelling is finished, it is saved as a “.stp” file and

added to the geometry of the static structural module. Figure 3.10 depicts a pictorial view of the sandwich structure modelling.

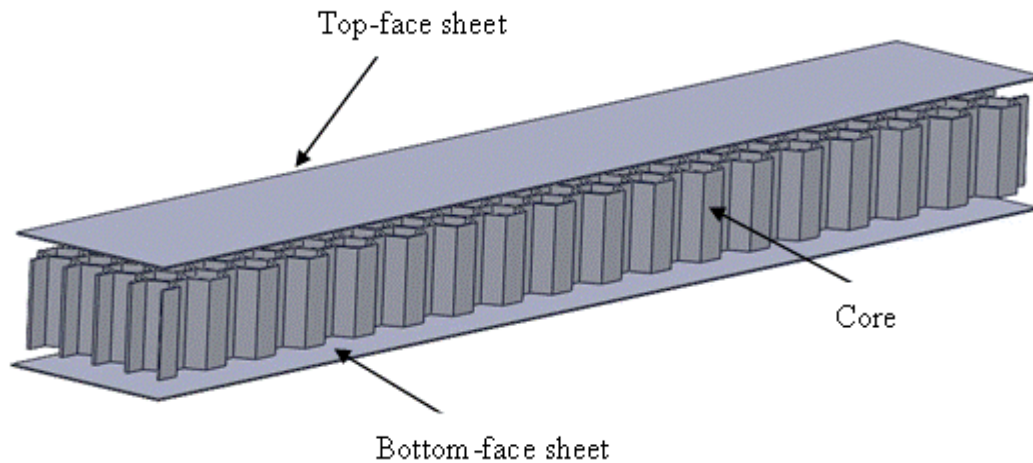


Fig. 3.10 Modelling of structure using SolidWorks.

3.7.2 Static structure module

This study is performed using the ANSYS Workbench module 'Static Structure.' Drag a static structural module to the project schematic window. The engineering material is first assigned. The geometry is then uploaded from where it was stored as a '.stp' file in Solidworks. The solver is then created. Figure 3.11 given below depicts the interface of the project schematic windows used in ANSYS Workbench 2022-R1.

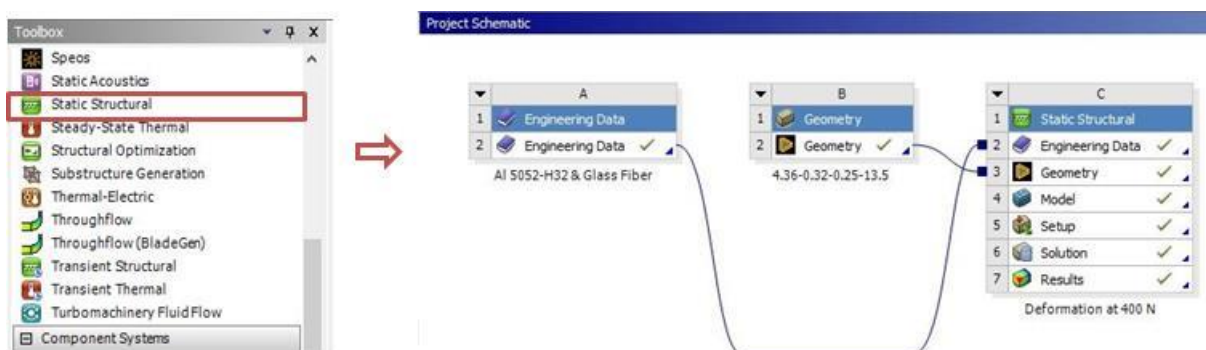


Fig. 3.11 Interface of project schematic window in ANSYS

3.7.3 Element type and Mesh size

The meshing type can be automated or the user can create a method for manually setting the meshing type. The same may be said about mesh size. By clicking on 'generate mesh' button, the ANSYS solver generates default mesh sizing. The second option is to

Materials and Methods...

right-click on 'mesh', then click on 'sizing' and then enter desired size (say 1mm) to generate mesh size. Here mesh size of model is taken as 4 mm through mesh convergence test.

3.7.4 Material model

In this study, an aluminium honeycomb core of Al 5052-H32 and glass fiber were employed for the face sheet. Material attributes are manually put into 'Engineering Data.' The structural steel used for the pusher member and supports is sourced from the ANSYS material database. The reason for choosing structural steel for pusher member and support was because of the high Young's Modulus due to which when the puller member pulls with some external force, there is no deformation generated in to these members. The table below displays various mechanical characteristics of materials. The mechanical properties of core and face sheet is given in the table below in table 3.1.

Table 3.1 Mechanical properties of material used.

S. N	Properties	Core Aluminium 5052-H32	Face sheet Glass Fiber
1.	Density	83 kg/mm ³	0.47 kg/m ³
2.	Poisson's ration	0.33	0.125
3.	Elongation (%)	13	4.8
4.	Tensile Modulus (GPa)	70.3	20
5.	Compressive Strength (MPa)	5.67	467
6.	Compressive Modulus (GPa)	1.31	17
7.	Shear Strength (MPa)	0.68	1.35
8.	Shear Modulus (MPa)	565	30,000

3.7.5 Boundary conditions

The boundary conditions were modified accordingly as the specimen was loaded with a three-point bend test. The sandwich panel was fixed in place by two supports placed at a 20 mm distance from both ends. Distance between two fixed supports is 140 mm. In the centre of the sandwich panel, a pusher member with a specified pushing force was acting in a negative Y direction. As previously stated, both the support and the pusher were composed of structural steel with maximum strength, therefore no strains were

created on either while applying force. The connections generated between the pusher and support members remained as frictionless contacts. Boundary conditions as shown in Fig. 3.12 depicts the constrains that were used in this analysis.

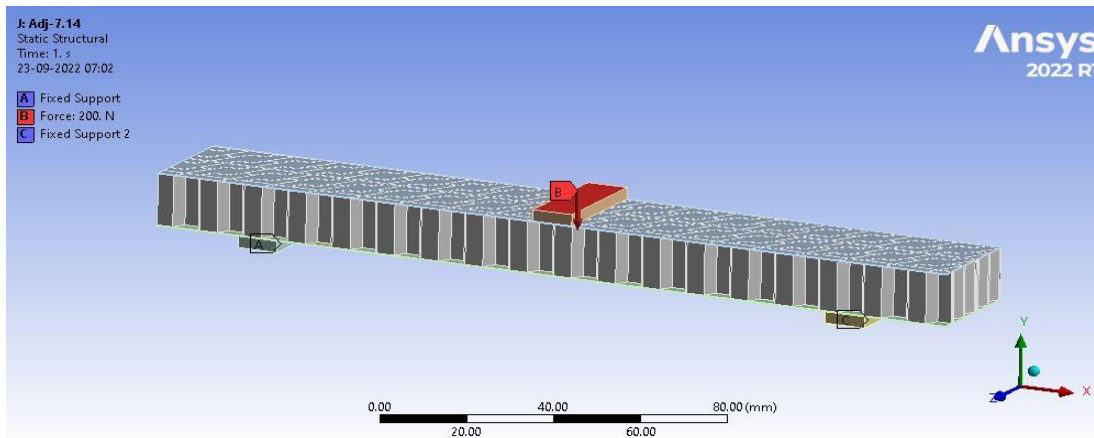


Fig. 3.12 Boundary conditions for honeycomb sandwich structure

3.7.6 Solver outcome

At a defined pushing force, there was an amount of deformation and stresses developed in the sandwich panel. That deformation an output in a solver, which was then compared to all results to obtain the best shape. To identify which is better suited, the outcomes of sub-structure and super-structure are compared.



Results
and
Discussion



Chapter 4

RESULT AND DISCUSSION

4.1 Introduction

The current study investigated the influence of sub-structure and super-structure geometry on the regular honeycomb structure. Following the introduction of geometry, the deformation and stresses are analyzed, and the influence of the newly added geometry is considered. The dimensions of the honeycomb sandwich panel are the same as those of the validated paper. The sub-structure is first introduced to the standard hexagonal honeycomb core, and then it is replaced by the super-structure. The size factors (α and β) are preserved in the first order. A honeycomb sandwich construction with a composite fiber face sheet and an Al 5052-H32 core is deformed by a downward pushing force. The maximum deflection is measured at the centre of the structure.

4.2 Validation using Finite Element Method

The experimental work of Hussain et al. (2018) is evaluated with finite element modelling using ANSYS Workbench 2022-R1. The honeycomb sandwich structure was put over two fixed supports in a three-point bend arrangement, and one pusher member applied forces of 200 N, 400 N, 600 N, 800 N, and 1000 N. The structure was deformed to an elastic state. Figure 4.1 shows a comparison of experimental and numerical force vs. displacement graph.

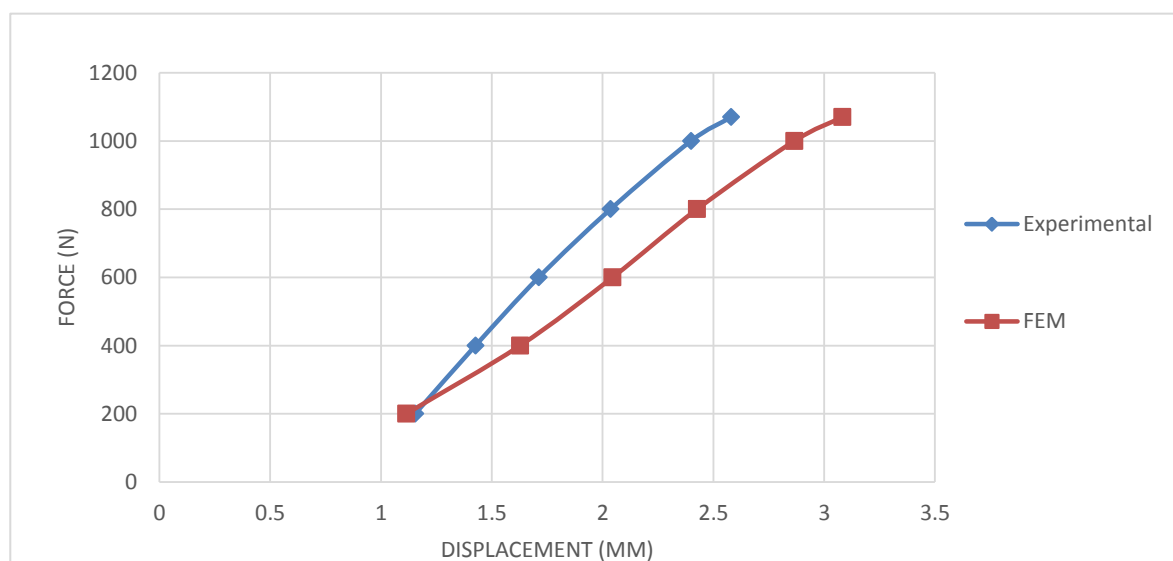


Fig. 4.1 Validation of experimental results with numerical results (Hussain et al. 2018)

When 200 N is applied in the negative Y direction, as illustrated in the graph above, there is initially a bigger amount of deflection than the experimental result. When the force increases from 400 n to 1000 n, the difference between the two lines is significant. The greatest variation between experimental and numerical results for validation is around 19%. As a result, the numerical modelling technique has been validated, and the numerical approach is acceptable and accurate.

4.3 Mesh convergence test

Mesh selection was made based on mesh convergence. Apart from other correct boundary conditions, meshing is the most crucial aspect in FEM to obtain accurate results. The force applied goes through these nodes, which are specified by the mesh size. As a result, the appropriate mesh size should be chosen based on mesh convergence criteria as well as processing time. Mesh convergence is depicted by the Fig. 4.2 below.

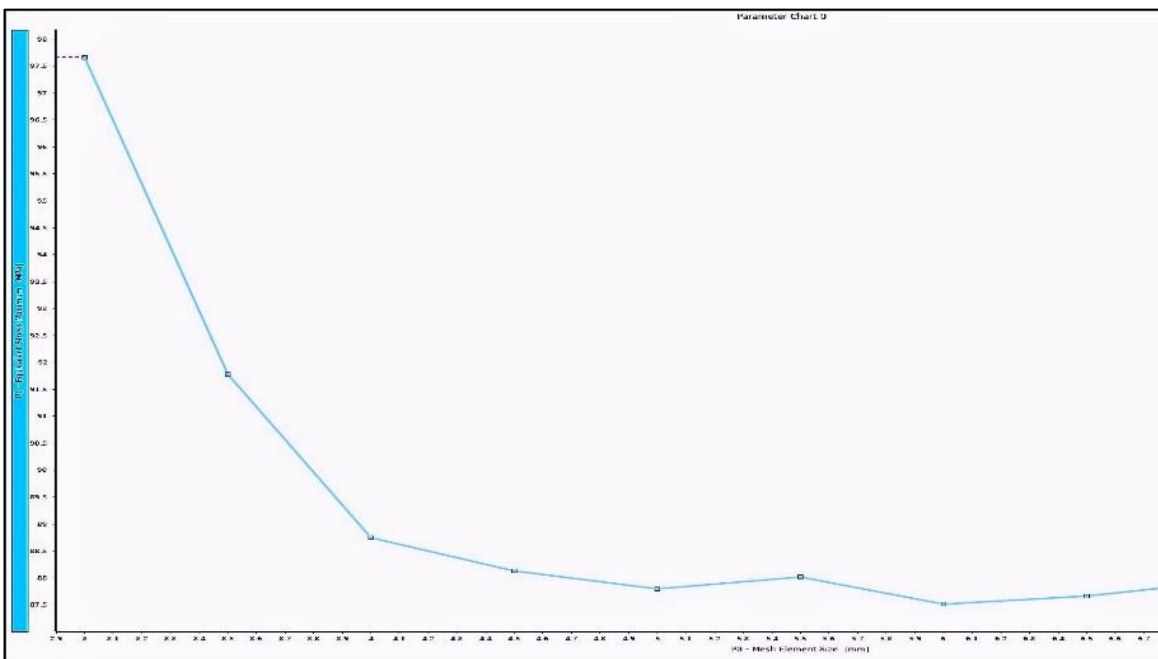


Fig. 4.2 Mesh convergence test performed in ANSYS

It is clear from the image that the mesh size begins at 8 and refined up to 3. When the mesh size reaches 5, the slope changes, indicating that the mesh solution is converging with regard to equivalent stresses created in the sandwich structure. So after mesh convergence test performed with in ANSYS workbench the mesh size can lie between 4 to 5 mm. Here for this numerical solution the mesh size was taken as 4 mm.

4.4 Effect of super-structure

With two alternative designs, a superstructure of various sizes was inserted into base geometry. First, the superstructures were placed next to each other, as seen in Fig. 4.3(a). The second way was to alternately implant the superstructure, as seen in Fig. 4.3 (b).

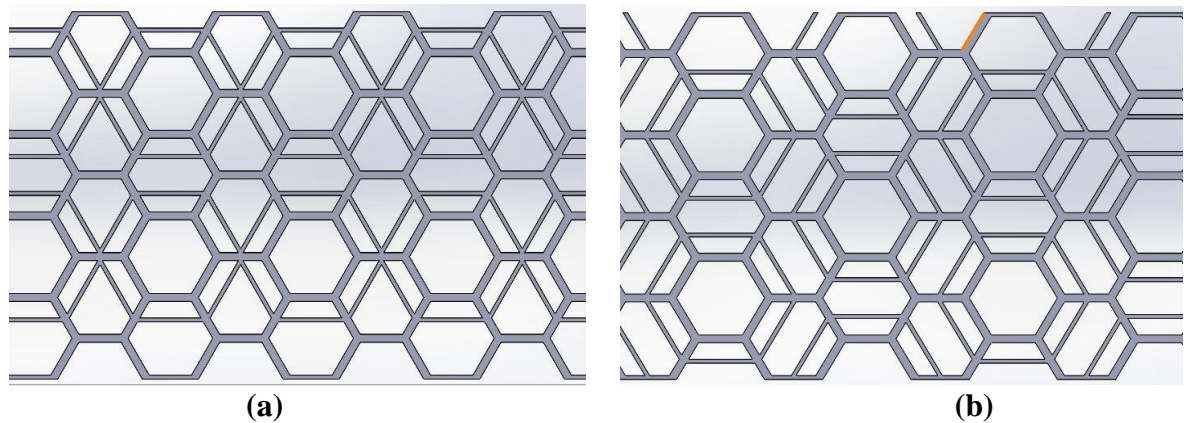


Fig. 4.3 (a) Placement of super-structure in adjacent pattern; (b) Placement of super-structure in alternate pattern.

4.4.1 Adjacent pattern

The adjacent pattern was modelled using core heights of 10 mm, 13.5 mm, and 15 mm, respectively. The sandwich construction was then loaded as a three-point bend specimen with the boundary condition. The pusher member was subjected to downward or negative y-direction forces of 200 N, 400 N, 600 N, 800 N, and 1000 N, respectively. The honeycomb sandwich construction is made of Al 5052-H32 as the core material and glass fibre composite as the facing sheet. The structural steel pusher member and support were used. The boundary condition are depicted in the Fig. 4.4 below.

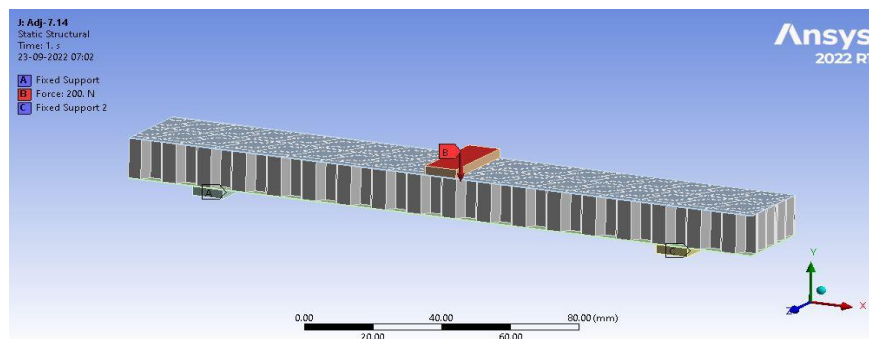


Fig. 4.4 Boundary conditions for super-structure with adjacent pattern honeycomb sandwich

The deflection was obtained as a solver output after applying boundary conditions. Figure 4.5 displays the numerically computed deflection in mm. The maximum deflection of 2.9833 mm was found for face length of the hexagonal superstructure was 7.14 mm.

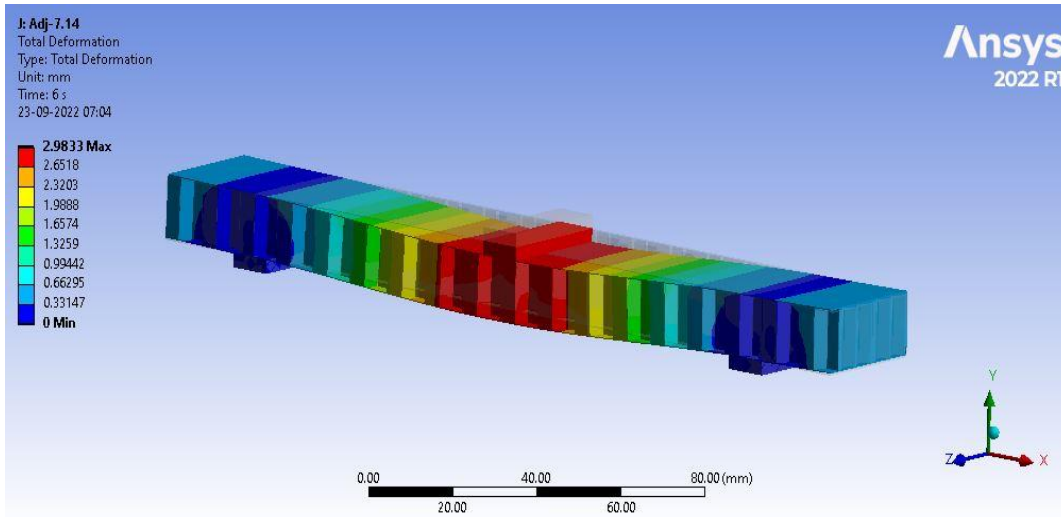


Fig. 4.5 Deflection as output for super-structure with adjacent pattern honeycomb sandwich

Figure 4.6 depicts a graph of force vs. displacement for cell height as 10 mm. In this case, four different cell lengths were chosen: 4.36 mm, 5.32 mm, 6.28 mm, and 7.14mm.

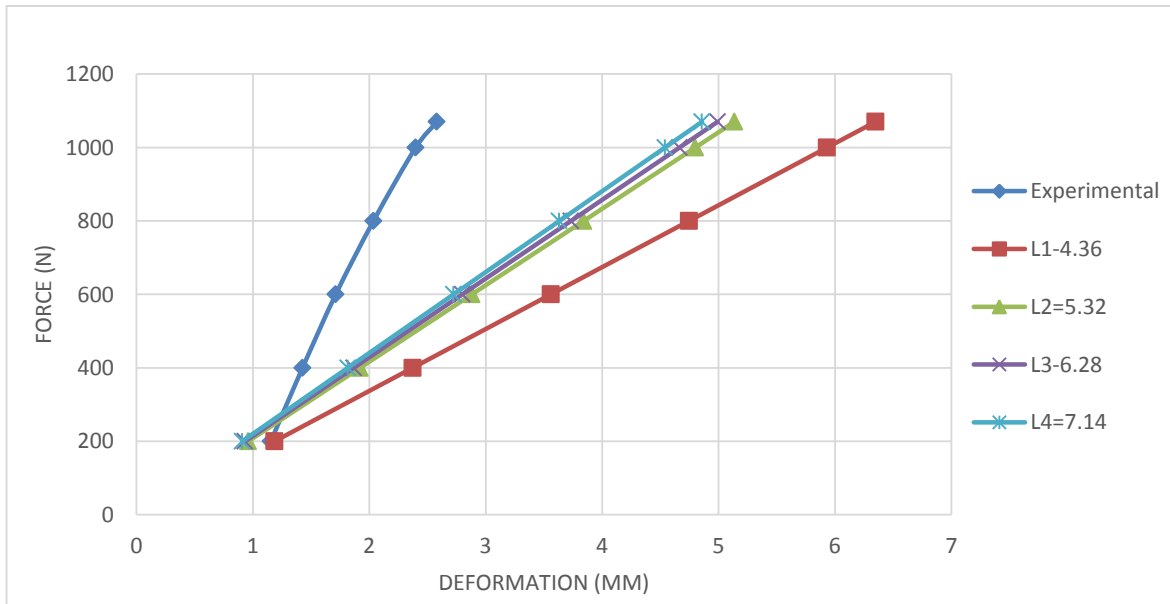


Fig. 4.6 Force vs. Displacement graph with cell height of 10mm

Figure 4.7 below depicts a graph of force vs. displacement for cell height as 13.5 mm.

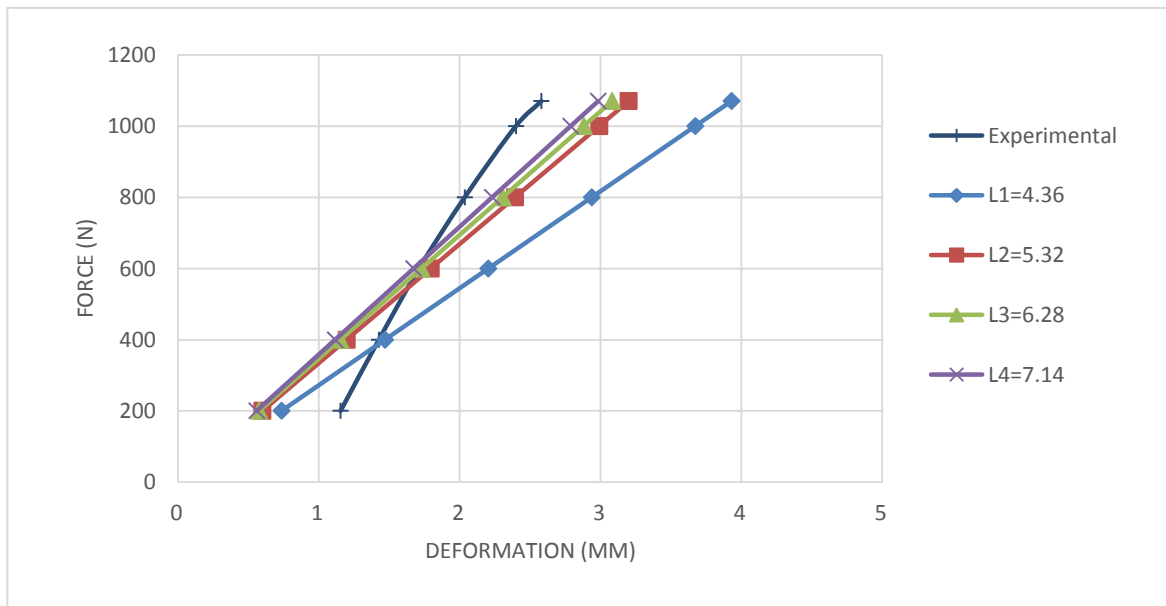


Fig. 4.7 Force vs. Displacement graph with cell height of 13.5 mm

Figure 4.8 below depicts a graph of force vs. displacement for cell height as 15 mm.

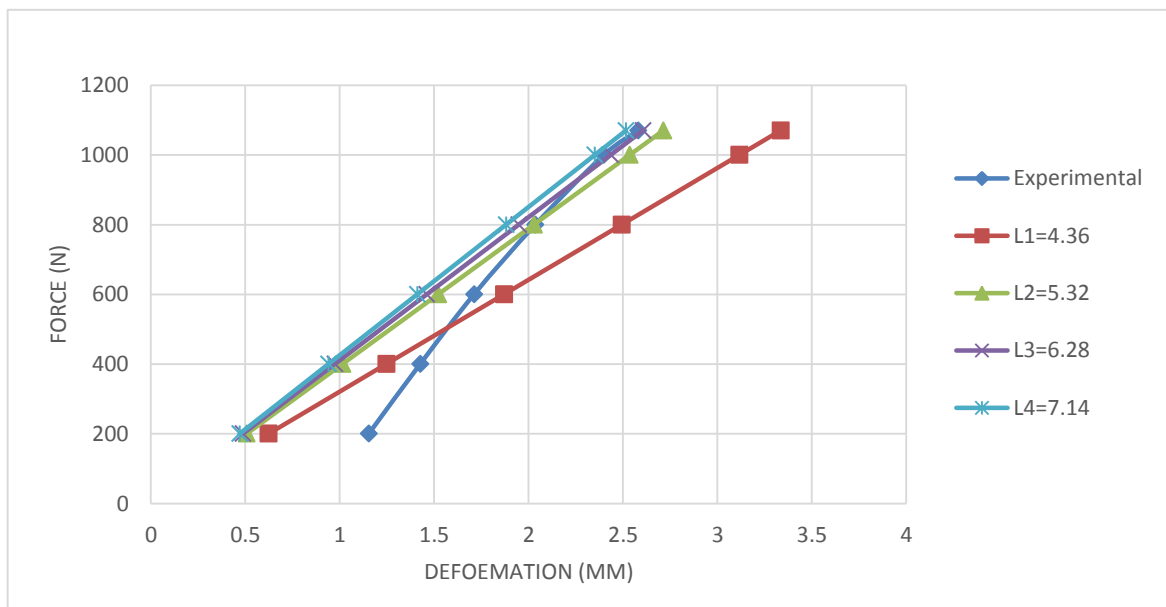


Fig. 4.8 Force vs. Displacement graph with cell height of 15 mm

When compared to the experimental geometry, which had a core height of 13.5 mm, the cell height of the core retained at 10 mm showed increased deformation in the

graph above as shown in Fig. 4.6. When the cell length was least i.e. 4.36 mm the deflection was maximum of 6.3481 mm. If the core height is reduced, it is expected that the superstructure will not function effectively. But as the core height was increased from 15 mm, it can be visualized that there is minimum deflection in the sandwich structure as 2.5155 mm.

4.4.2 Alternate pattern

The superstructure was inserted alternately after leaving one hexagonal cell in the alternate arrangement. The major reason for doing this was to construct a cross ribbon to increase the structure's load bearing capability. Long horizontal ribbons were developed in the adjacent pattern. These ribbons were used to strengthen the conventional hexagonal cell. The boundary conditions were likewise maintained constant in this case. The force was applied in the same manner, with increments of 200 N, 400 N, 600 N, 800 N, and 1000 N in negative y-direction. The boundary conditions are depicted in the Fig. 4.9 below.

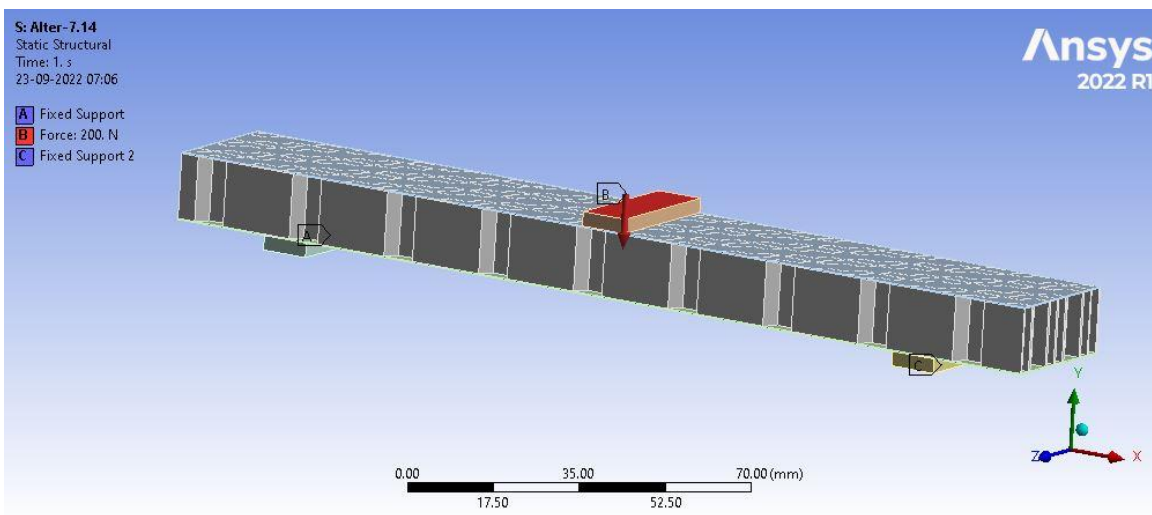


Fig. 4.9 Boundary conditions for super-structure with alternate pattern honeycomb sandwich

The deflection was obtained as a solver output after applying boundary conditions. Figure 4.10 displays the numerically computed deflection in mm. The maximum deflection of 3.0199 mm was found for face length of the hexagonal superstructure was 7.14 mm.

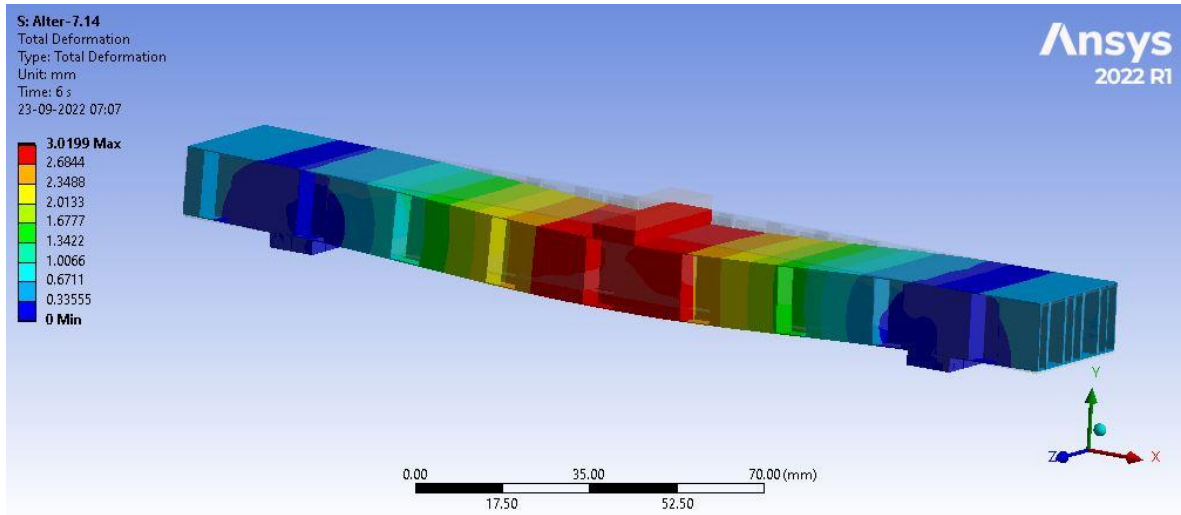


Fig. 4.10 Deflection as output for super-structure with alternate pattern honeycomb sandwich.

Figure 4.11 depicts a force vs. displacement graph for cell height as 10 mm.

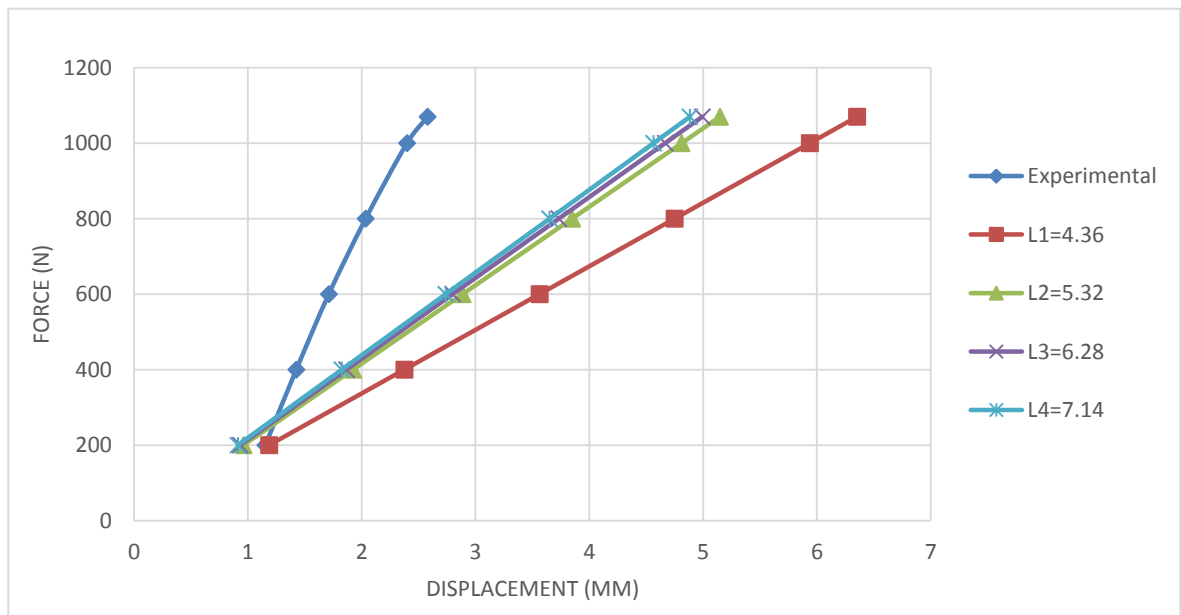


Fig. 4.11 Force vs. Displacement graph with cell height of 10mm.

Figure 4.12 below depicts a force vs. displacement graph for cell height as 13.5 mm.

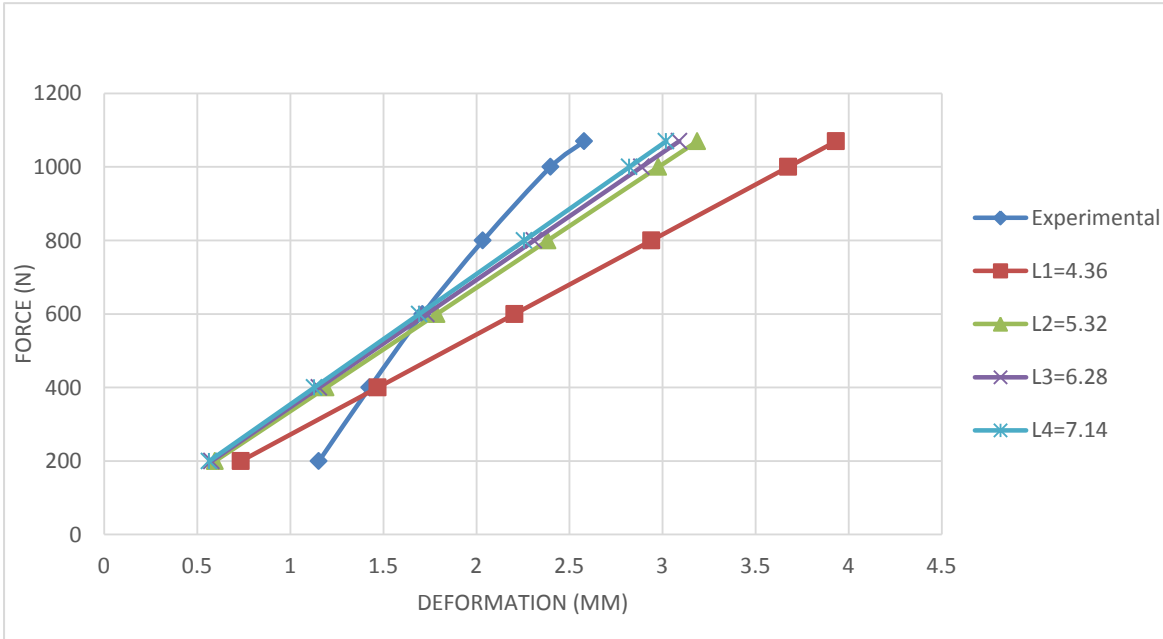


Fig. 4.12 Force vs. Displacement graph with cell height of 13.5 mm

Figure 4.13 below depicts a force vs. displacement graph for cell height as 15 mm.

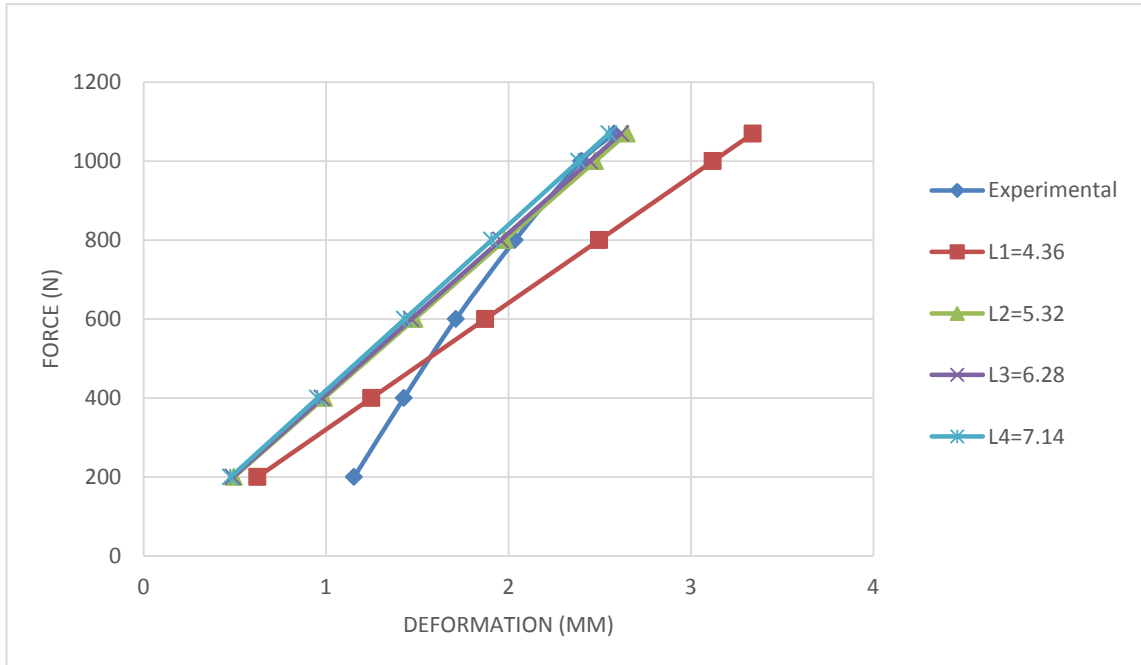


Fig. 4.13 Force vs. Displacement graph with cell height of 15 mm

In alternate geometry pattern, when the cell length was least i.e. 4.36 mm with cell height of 10 mm, the deflection was maximum of 6.3536 mm. If the core height is

reduced, it is expected that the superstructure will not function effectively. But as the core height was increased from to 15 mm, it can be visualized that there is minimum deflection in the sandwich structure as 2.5511 mm.

When comparing adjacent and alternate geometry super-structure patterns, it was discovered that there is not a significant difference when examining the deflection. When the cell height was 10 mm, the adjacent pattern deformed by 4.8582 mm, whereas the alternate pattern deformed by 4.8841 mm. The same thing happened with a 13.5 mm cell height. The adjacent pattern deformed by 2.9833 mm, whereas the other pattern deformed by 3.0199 mm. Finally, when the cell height was 15 mm, the adjacent pattern deformed by 2.5155 mm, whereas the alternate pattern deformed by 2.5511 mm. So it can be concluded that when comparing both adjacent and alternate patterns, the adjacent pattern performed better. This was due to the horizontal cell walls created at joining of two super-structures. The super-structure walls was ribbon reinforced, which helped in maintaining the maximum stiffness of the structure.

4.4.3 Face sheet thickness variation

The thickness of the face sheets has a greater influence on the rigidity of a honeycomb sandwich structure. The thickness of the face sheet reduces the overall deformation of a honeycomb sandwich construction (Ugur et al. 2020). In this case, three variants of face sheet thickness were considered: 0.25 mm, 0.50 mm, and 0.75 mm as shown in Fig. 4.14. These thicknesses were compared to the calculated deformation based on the experimental data.

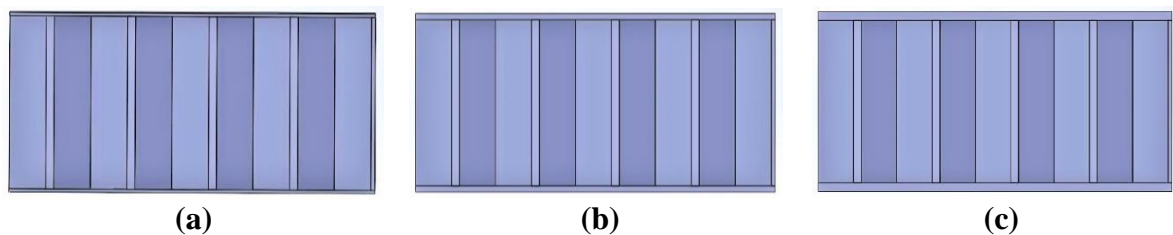


Fig. 4.14 (a) Sandwich structure with core height of 13.5 mm and face sheet height with 0.25 mm each; (b) Sandwich structure with core height of 13.5 mm and face sheet height with 0.50 mm each; (c) Sandwich structure with core height of 13.5 mm and face sheet height with 0.75 mm each

Firstly, the core height is kept as 10 mm and then thickness of face sheet is increased as 0.25 mm, 0.5 mm, 0.75 mm. There is also the variation of super-structure cell length as 4.36 mm, 5.32 mm, 6.28 mm, and 7.14mm.

Figure 4.15 depicts the force vs. displacement graph of super-structure cell length as 4.36mm and face sheet variation as 0.25 mm, 0.5 mm, 0.75 mm.

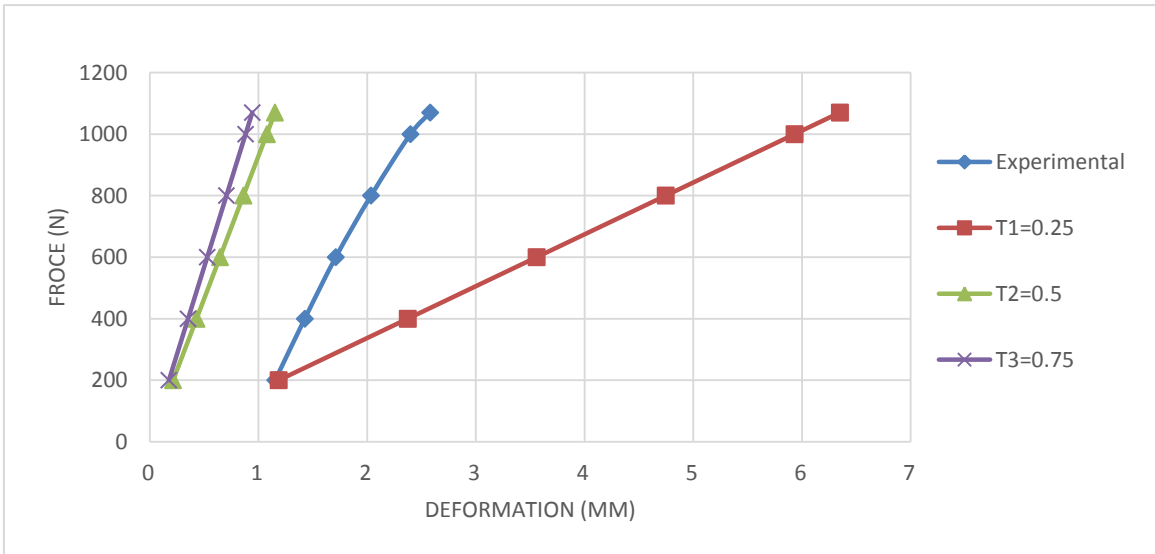


Fig. 4.15 Force vs. Displacement graph with cell length as 4.36 mm and cell height as 10 mm

Figure 4.16 depicts the force vs. displacement graph of super-structure cell length as 5.32mm and face sheet variation as 0.25 mm, 0.5 mm, 0.75 mm.

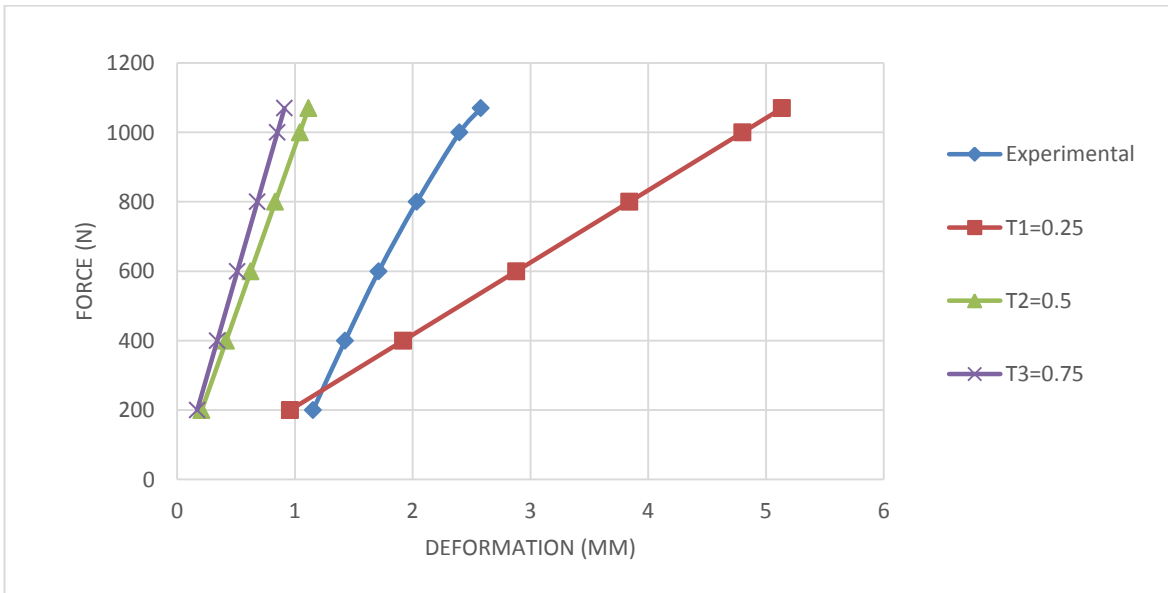


Fig. 4.16 Force vs. Displacement graph with cell length as 5.32 mm and cell height as 10 mm

Figure 4.17 depicts the force vs. displacement graph of super-structure cell length as 6.28 mm and face sheet variation as 0.25 mm, 0.5 mm, 0.75 mm.

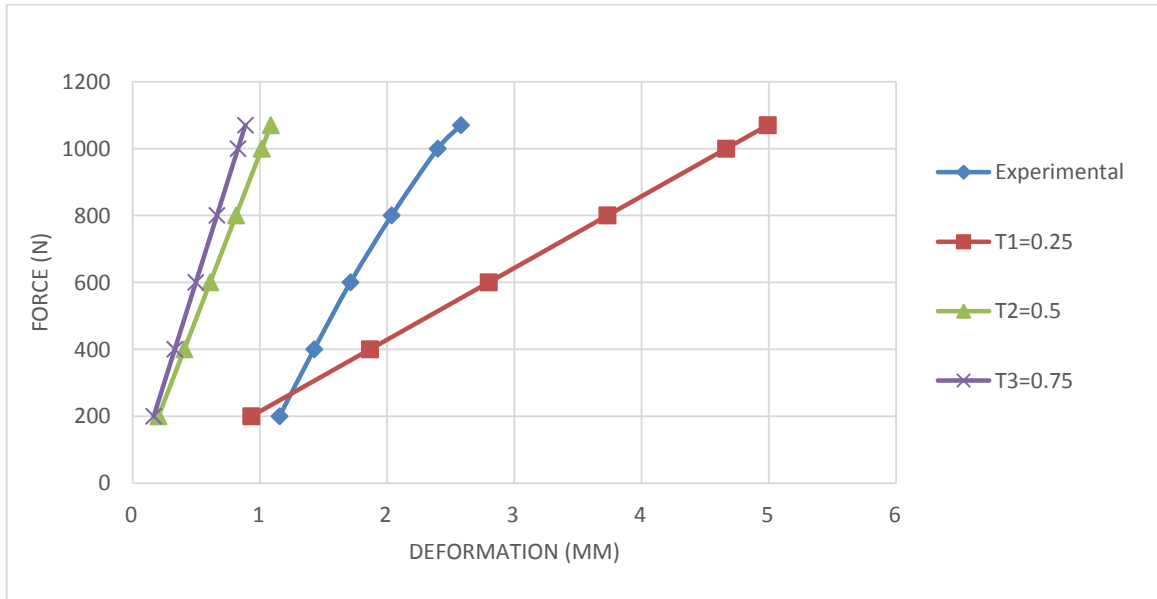


Fig. 4.17 Force vs. Displacement graph with cell length as 6.28 mm and cell height as 10 mm

Figure 4.18 depicts the force vs. displacement graph of super-structure cell length as 7.14 mm and face sheet variation as 0.25 mm, 0.5 mm, 0.75 mm.

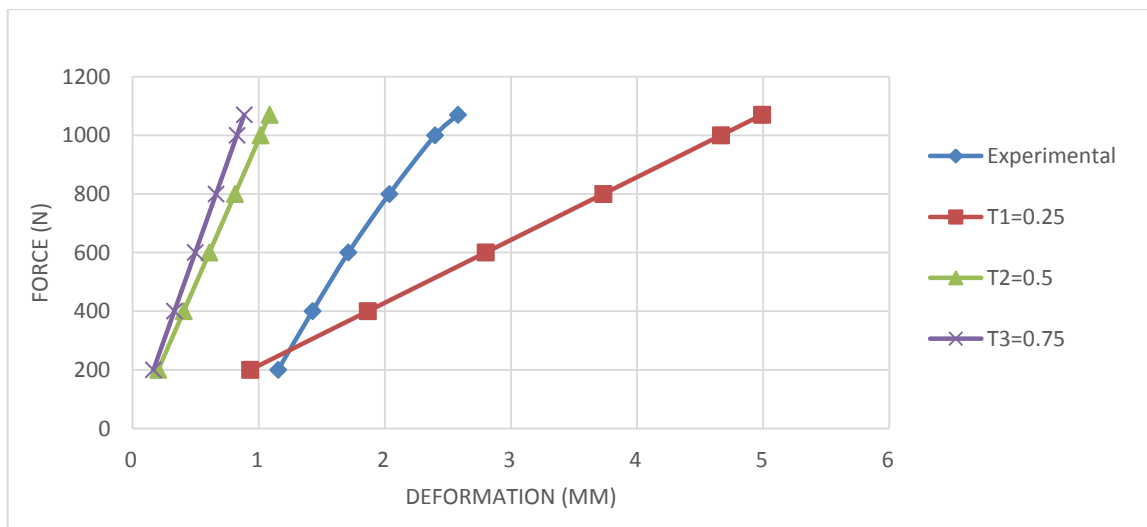


Fig. 4.18 Force vs. Displacement graph with cell length as 7.14 mm and cell height as 10 mm

The graphs show that the thickness of the face sheet is critical in preserving the stiffness of the honeycomb structure. When the cell length is 4.36 mm, cell height as 10 mm and with a face sheet thickness of 0.25 mm, the deformation is 6.3481 mm, but when the face sheet thickness is changed to 0.75 mm, the deformation is 0.94366 mm.

Now the core height is kept as 13.5 mm and then thickness of face sheet is increased as 0.25 mm, 0.5 mm, 0.75 mm. There is also the variation of super-structure cell length as 4.36 mm, 5.32 mm, 6.28 mm, and 7.14mm.

Figure 4.19 depicts the force vs. displacement graph of super-structure cell length as 4.36 mm and face sheet variation as 0.25 mm, 0.5 mm, 0.75 mm.

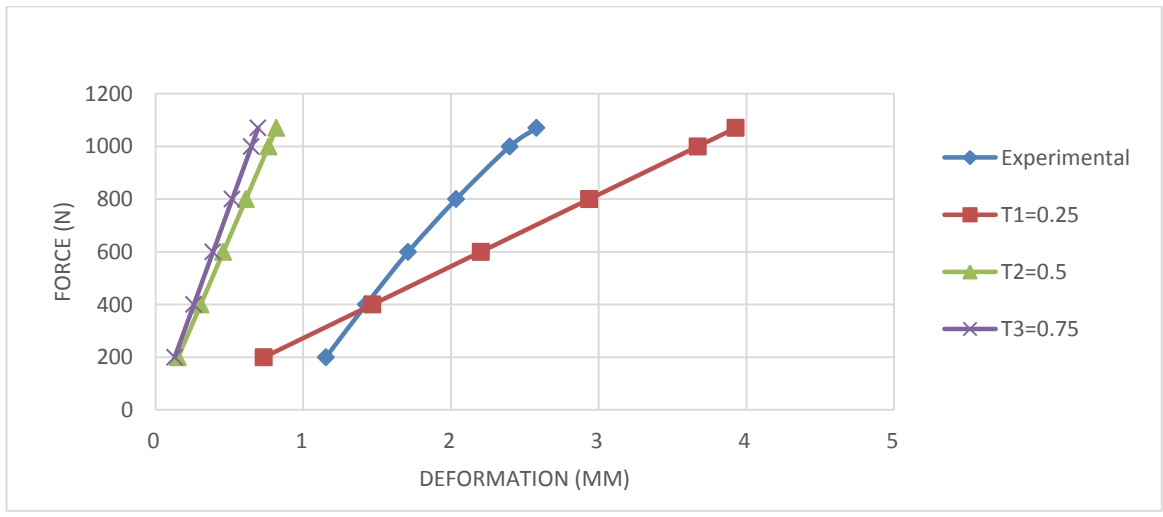


Fig. 4.19 Force vs. Displacement graph with cell length as 4.36 mm and cell height as 13.5 mm

Figure 4.20 depicts the force vs. displacement graph of super-structure cell length as 5.32 mm and face sheet variation as 0.25 mm, 0.5 mm, 0.75 mm.

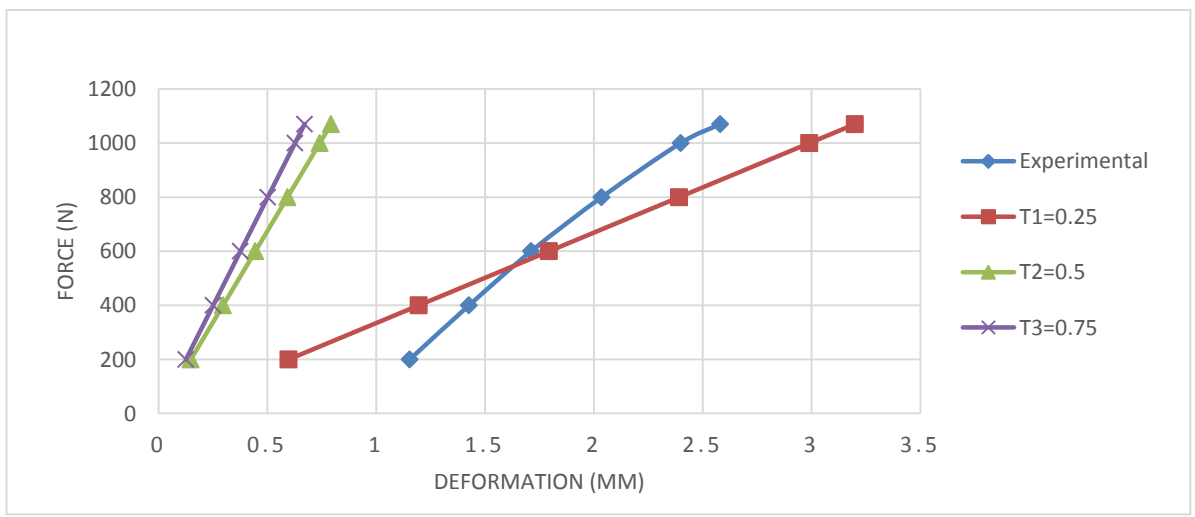


Fig. 4.20 Force vs. Displacement graph with cell length as 5.32 mm and cell height as 13.5 mm

Figure 4.21 depicts the force vs. displacement graph of super-structure cell length as 6.28 mm and face sheet variation as 0.25 mm, 0.5 mm, 0.75 mm.

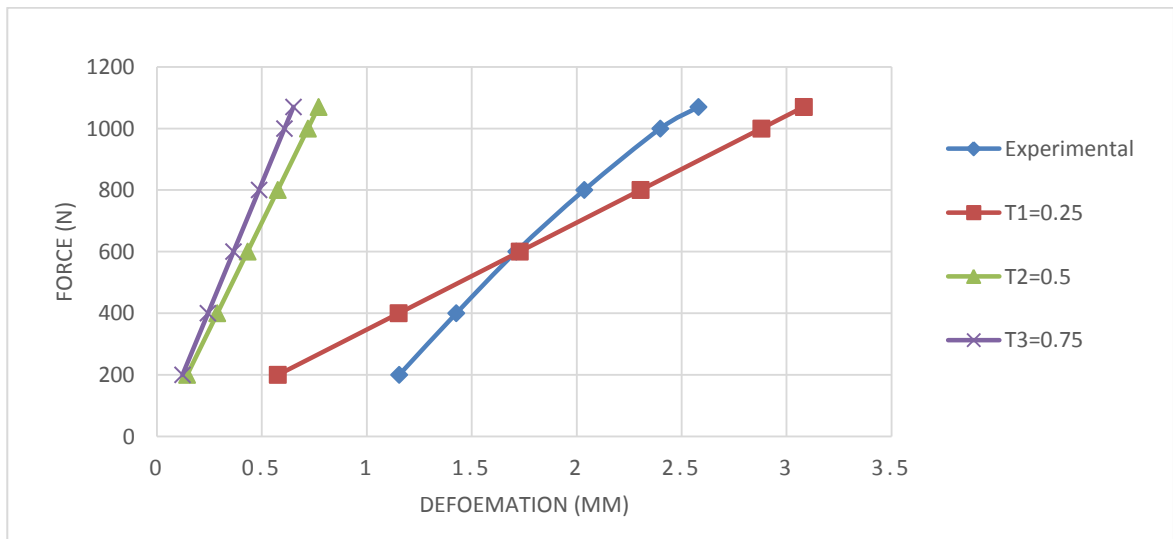


Fig. 4.21 Force vs. Displacement graph with cell length as 6.28 mm and cell height as 13.5 mm

Figure 4.22 depicts the force vs. displacement graph of super-structure cell length as 7.14 mm and face sheet variation as 0.25 mm, 0.5 mm, 0.75 mm.

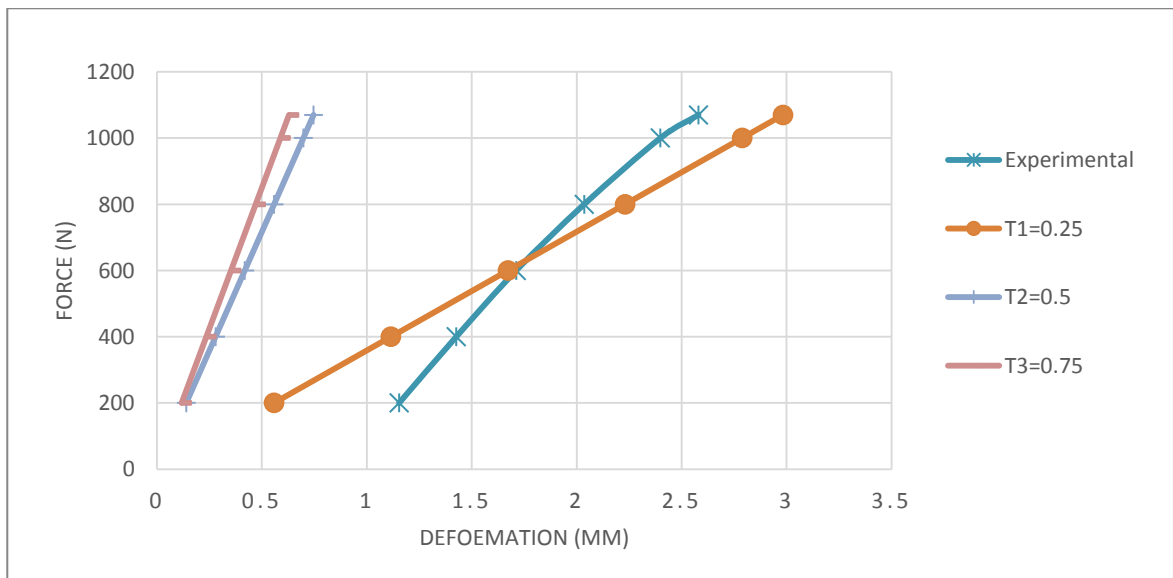


Fig. 4.22 Force vs. Displacement graph with cell length as 7.14 mm and cell height as 13.5 mm

When cell length is 5.32 mm, cell height as 13.5 mm and with a face sheet thickness of 0.25 mm, the deformation is 5.1368 mm, but when the face sheet thickness is changed to 0.75 mm, the deformation is 0.9113 mm. Now the core height is kept as 15 mm and then thickness of face sheet is increased as 0.25 mm, 0.5 mm, 0.75 mm. There is also the variation of super-structure cell length as 4.36 mm, 5.32 mm, 6.28 mm, and 7.14mm.

Figure 4.23 depicts the force vs. displacement graph of super-structure cell length as 4.36 mm and face sheet variation as 0.25 mm, 0.5 mm, 0.75 mm.

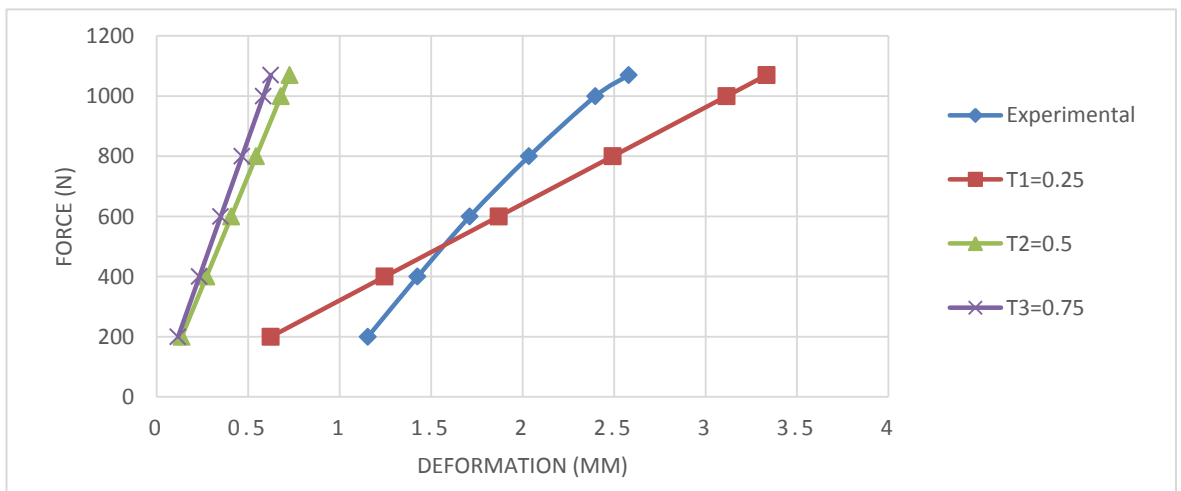


Fig. 4.23 Force vs. Displacement graph with cell length as 4.36 mm and cell height as 15 mm

Figure 4.24 depicts the force vs. displacement graph of super-structure cell length as 5.32 mm and face sheet variation as 0.25 mm, 0.5 mm, 0.75 mm.

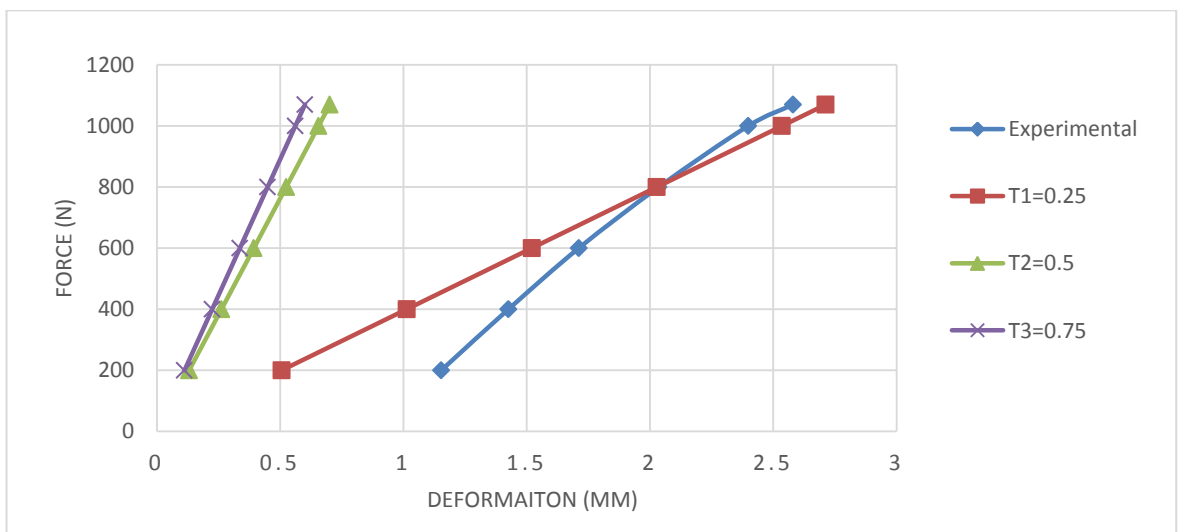


Fig. 4.24 Force vs. Displacement graph with cell length as 5.32 mm and cell height as 15 mm

Figure 4.25 depicts the force vs. displacement graph of super-structure cell length as 6.28 mm and face sheet variation as 0.25 mm, 0.5 mm, 0.75 mm.

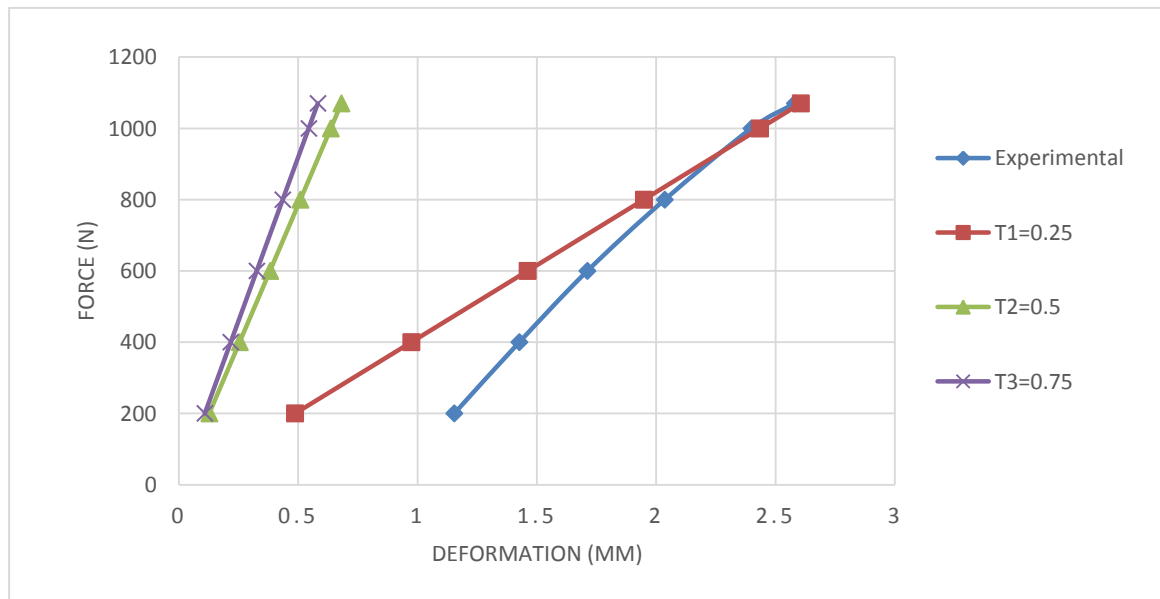


Fig. 4.25 Force vs. Displacement graph with cell length as 6.28 mm and cell height as 15 mm

Figure 4.26 depicts the force vs. displacement graph of super-structure cell length as 7.14 mm and face sheet variation as 0.25 mm, 0.5 mm, 0.75 mm.

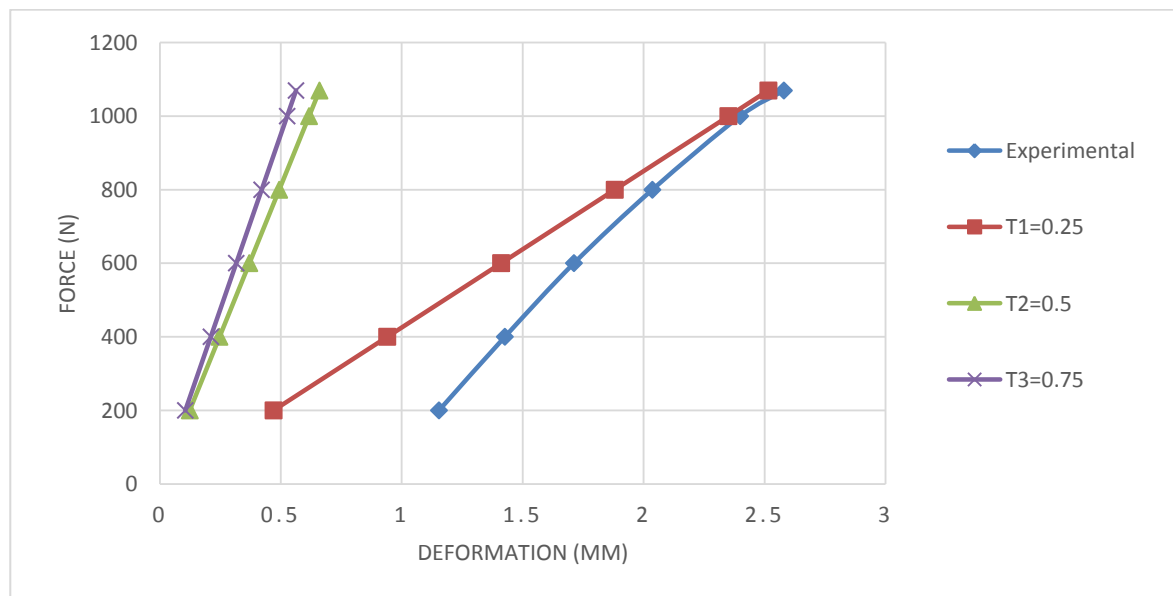


Fig. 4.26 Force vs. Displacement graph with cell length as 7.14 mm and cell height as 15 mm

This determines that the core height and face sheet of any sandwich construction are the parameters that affect the mechanical characteristics of the structure. We can adjust the thickness of the face sheet if we don't want to change the core height. This changes the stiffness requirement of any structure. The optimum methodology is to optimize both parameters and select a shape with increased cell height and face sheet thickness.

4.4.4 Super-structure wall thickness variation

A honeycomb structure is made up of numerous cells that are linked to one another, so a stiffer material by optimizing cell wall thickness may be obtained. The variation in cell wall thickness is taken into account in this numerical approach. The geometry of the superstructure is doubled to 0.64 mm in this case. Keeping the boundary condition constant, the applied force in the negative y direction was calibrated at 200 N, 400 N, 600 N, 800 N, and 1000 N. To begin with, the superstructure's cell wall was retained at its initial thickness of 0.32 mm. After that cell wall thickness was then doubled. A solution was found, and graphs were created.

Figure 4.27 depicts the thickness variation of super-structure wall thickness.

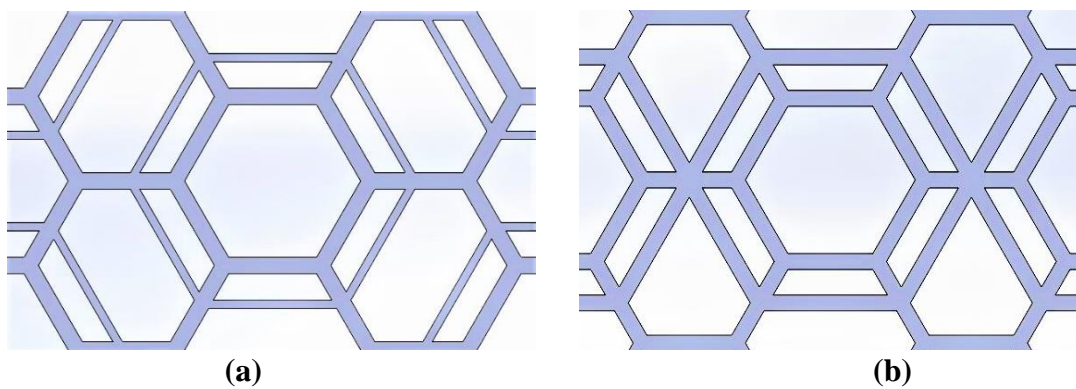


Fig 4.27 (a) Super-structure cell wall thickness as 0.32 mm; (b) Super-structure cell wall thickness as 0.64 mm

Figure 4.28 depicts the force vs. displacement graph of super-structure cell length as 4.36 mm and cell wall thickness variation as 0.32 mm and 0.64 mm.

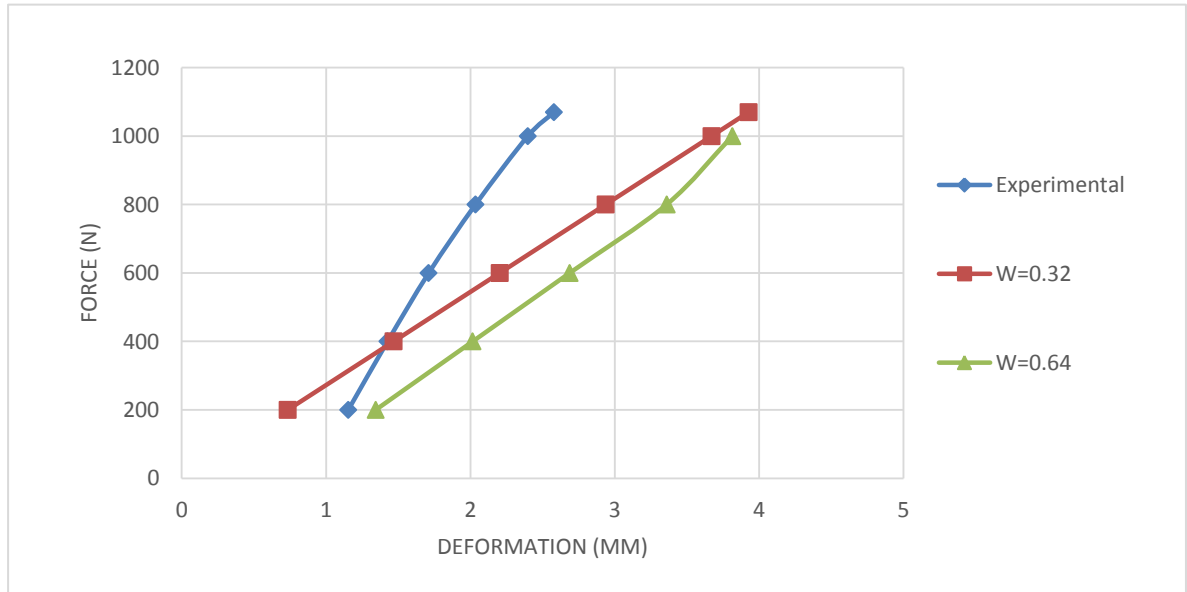


Fig. 4.28 Force vs. Displacement graph with cell length as 4.36 mm and cell height as 13.5 mm

Figure 4.29 depicts the force vs. displacement graph of super-structure cell length as 5.32 mm and cell wall thickness variation as 0.32 mm and 0.64 mm.

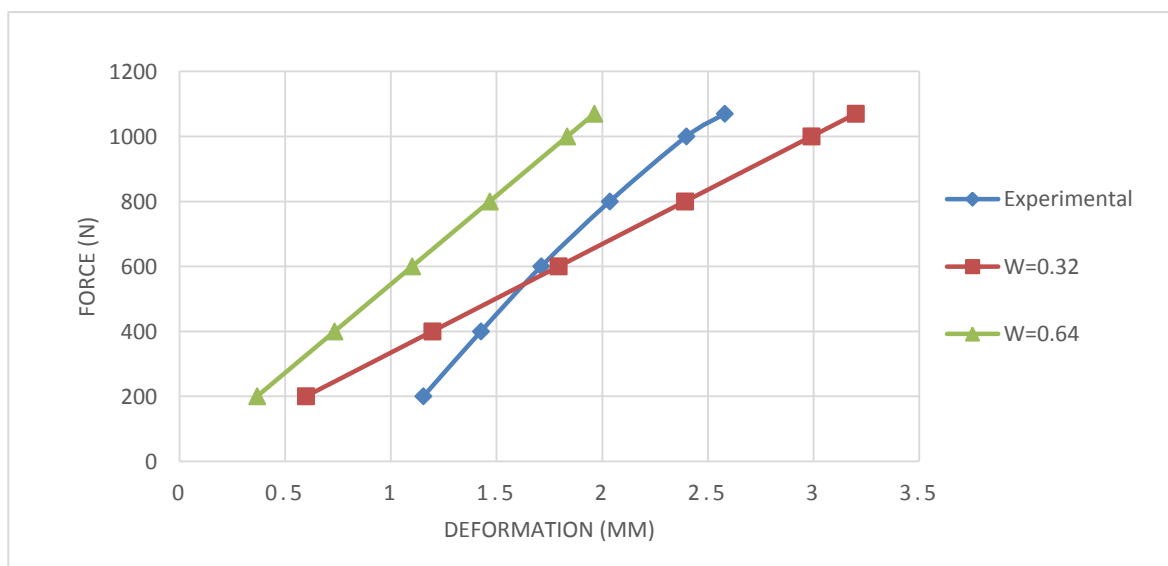


Fig. 4.29 Force vs. Displacement graph with cell length as 5.32 mm and cell height as 13.5 mm

When the width of the superstructure was 0.32 mm, the maximum deformation was 3.9292, but when the width was increased to 0.64 mm, the maximum deformation was 3.8155. When a cell wall length of 5.32 mm was investigated, the same result was

obtained. The deformation achieved when the cell wall thickness was 0.32 mm was 3.1997 mm, but when the thickness was altered to 0.64 mm, the deformation decreased to 1.9628 mm.

This study revealed that cell wall thickness effects the mechanical qualities of the structure. The material behaviour does not change when the cell wall thickness of a superstructure is kept constant, i.e. 0.32 mm. However, when the wall thickness was doubled, i.e., 0.64, the findings changed dramatically and the stiffness of the material improved. This enhances the material's load bearing capability.



Summary
and
Conclusion



Chapter 5 **SUMMARY AND CONCLUSIONS**

5.1 General

The current study utilizes a static module to analyze deformation on a hexagonal honeycomb sandwich construction. The deformation of a standard sandwich structure is examined after a superstructure is inserted. Geometrical modifications of the superstructure are then considered in order to improve mechanical qualities.

The conclusions of the investigations are summarized as follows:

1. All super-structure geometries were modelled, numerically analyzed and results were obtained.
2. When super-structure are placed using adjacent pattern, it was observed that when core height was least i.e., 10 mm, the maximum deformation was 4.8581 mm but when the core height was 15 mm, the deformation observed was 2.516 mm which was lower than experimental result which was 2.5802 mm modeling modelling
3. When super-structure are placed using alternate pattern, it was observed that when core height was least i.e., 10 mm, the maximum deformation was 4.8841 mm but when the core height was 15 mm, the deformation observed was 2.551 mm which lower than experimental result which was 2.5802 mm modeling modelling
4. When both adjacent and alternate patterns were used, adjacent geometry pattern performed better with less deformation than alternative.
5. When face sheet thickness was considered, it was observed that when cell length was least i.e., 4.36 mm with face sheet thickness of 0.25 mm the deformation observed was 6.3481 mm. But when the face sheet was increased to 0.75 mm i.e., 3 times then the deformation increased up to 0.9436 mm.
6. When the face sheet thickness is increased than load bearing capacity of the structure gets improved.
7. When width of super-structure cell wall increased from 0.32 mm to 0.64 mm, then the deformation which was analyzed earlier 3.1997 mm decreased to 1.9628 mm.
8. Cell wall thickness of super-structure enhanced the mechanical properties of the structure.

5.2 Recommendation for future work

According to the findings, the addition of sub-structures and super-structures enhanced the load bearing capability of the standard honeycomb sandwich construction. This approach can be used as an alternative to strengthen the structure. Because metal 3D printing is becoming more popular, it is now possible to create a complicated shaped honeycomb core. There are several future possibilities for current work, including:

1. Hierarchical sub-structures of 2nd order and hierarchical super-structure of 2nd order can be used for in geometry modelling.
2. Combined effect of both 1st order sub-structure and 1st order super-structure can be evaluated.
3. For in-plane loading condition hierarchical structure can be replaced by re-entrant honeycomb cell.
4. For numerical analysis ANSYS Workbench can be replaced by Altair HyperMesh.



Literature Cited



LITERATURE CITED

A. Journal Articles

- Abbadi, A., Tixier, C., Gilgert, J. and Azari, Z. 2015.** Experimental study on the fatigue behaviour of honeycomb sandwich panels with artificial defects. *J. Compos. Struct.*, 120(1): 394-405.
- Ajdari, A., Jahromi, B., Papadopoulos, J., Nayeb-Hashemi, H. and Vaziri, A. 2012.** Hierarchical honeycombs with tailorable properties. *Int. J. Solids Struct.*, 49(2): 1413-1419.
- Aktay, L., Johnson, A. and Kroplin, B. 2008.** Numerical modelling of honeycomb core crush behaviour. *J. Eng. Fract. Mech.*, 75(9): 2616-2630.
- Ali, K. A., Kumar, S. S., Jeffrey, J. A., Ravikumar, M. M. and Rajkumar, S. 2021.** An insight into stress and strain analysis over on hexagonal aluminium sandwich honeycomb with various thickness glass fiber face sheets. *J. Mater. Today*, 47(1): 493-499.
- Chandrashekhar, A., Shaik, H. S., Mishra, S. R., Srivastava, T. and Kishore, M. L. 2021.** Static Structural Analysis of Hybrid Honeycomb Structures Using FEA. *J. Mech. Eng.*, 42(2): 363-375.
- Chawla, A., Mukherjee, S., Kumar, D., Nakatani, T. and Ueno, M. 2003.** Prediction of crushing behaviour of honeycomb structures. *Int. J. Crashworthiness*, 8(3): 229-235.
- Chen, Q. and Pugno, N. M. 2012.** In-plane elastic buckling of hierarchical honeycomb materials. *Eur. J. Mech. A Solids.*, 34(1): 120-129.
- Ciepielewski, R., Gieleta, R. and Miedzinska, D. 2022.** Experimental Study on Static and Dynamic Response of Aluminium Honeycomb Sandwich Structures. *J. Materials*, 15(5): 1793-1807.
- Dhari, R. S., Javanbakht, Z. and Hall, W. 2021.** On the deformation mechanism of re-entrant honeycomb auxetics under inclined static loads. *J. Mater. Lett.*, 286(1): 129-138.

- Ghaedizadeh, A., Shen, J., Ren, X. and Xie, Y. M. 2016.** Tuning the performance of metallic auxetic metamaterials by using buckling and plasticity. *Materials*, 9(1): 54-65.
- Ghongade, G., Kalyan, K. P., Vignesh, R. V. and Govindaraju, M. 2021.** Design, fabrication, and analysis of cost effective steel honeycomb structures. *J. Mater. Today*, 46(1): 4520-4526.
- Gibson, L. J. and Ashby, M .F. 1997.** The effects of non-periodic microstructure and defects on the compressive strength of two-dimensional cellular solids. *Int. J. Mech. Sci.*, 39(5): 549-563.
- Hussain, M., Khan, R. and Abbas, N. 2019.** Experimental and computational studies on honeycomb sandwich structures under static and fatigue bending load. *J. King Saud. Univ. Sci.*, 31(2): 222-229.
- Hong, S. T., Pan, J., Tyan, T. and Prasad, P. 2006.** Quasi-static crush behaviour of aluminium honeycomb specimens under compression dominant combined loads. *Int. J. Plast.*, 22(1): 73-109.
- Ingrole, A., Hao, A. and Liang, R. 2017.** Design and modelling of auxetic and hybrid honeycomb structures for in-plane property enhancement. *J. Mater. Des.*, 117(1): 72-83.
- Joshilkar, P., Deshpande, R. D. and Kulkarni, R. B. 2018.** Analysis of honeycomb structure. *Int. J. Res. Appl. Sci. Eng. Technol.*, 6(5): 950-958.
- Jiang, F., Yang, S., Ding, C. and Qi, C. 2022.** Quasi-static crushing behavior of novel circular double arrowed auxetic honeycombs: Experimental test and numerical simulation. *Thin Walled Struct.*, 177(1): 109-134.
- Kaveloglu, S. and Temiz, S. 2022.** An experimental and finite element analysis of 3D printed honeycomb structures under axial compression. *Polym. Polym. Compos.*, 30(1): 121-133.
- Lubis, S., Siregar, A. M. and Siregar, I. 2021.** Study of Statically Tested Honeycomb Structure. *Int. J. Eco. Technol. Soc. Sci.*, 2(1): 1-12.

- Mousanezhad, D., Babae, S., Ebrahimi, H., Ghosh, R., Hamouda, A. S., Bertoldi, K. and Vaziri, A. 2015.** Hierarchical honeycomb auxetic metamaterials. *Sci. Rep.*, 5(1): 1-8.
- Nazeer, S., Allabakshu, S. and Sergio, P. G. 2015.** Design and Analysis of Honey Comb Structures with Different Cases. *Int. J. Eng. Res. Dev.*, 3(4): 144-156.
- Onyibo, E. C. and Safaei, B. 2022.** Application of finite element analysis to honeycomb sandwich structures. *J. Mech. Eng.*, 3(1): 283-300.
- Peng, X. L. and Bargmann, S. 2021.** A novel hybrid-honeycomb structure: Enhanced stiffness, tunable auxeticity and negative thermal expansion. *Int. J. Mech. Sci.*, 190(1): 106-121.
- Taylor, C. M., Smith, C. W., Miller, W. and Evans, K. E. 2011.** The effects of hierarchy on the in-plane elastic properties of honeycombs. *Int. J. Solids Struct.*, 48(9): 1330-1339.
- Qin, Q., Xia, Y., Li, J., Chen, S., Zhang, W., Li, K. and Zhang, J. 2020.** On dynamic crushing behavior of honeycomb-like hierarchical structures with perforated walls: Experimental and numerical investigations. *Int. J. Impact Eng.*, 145(1): 103-114.
- Rao, K. K., Rao, K. J., Sarwade, A. G. and Chandra, M. S. 2012.** Strength analysis on honeycomb sandwich panels of different materials. *Int. J. Eng. Res. Appl.*, 2(3): 365-374.
- Ugur, L., Duzcukoglu, H., Sahin, O. S. and Akkus, H. 2020.** Investigation of impact force on aluminium honeycomb structures by finite element analysis. *J. Sandw. Struct. Mater.*, 22(1): 87-103.
- Upreti, S., Singh, V. K., Kamal, S. K., Jain, A. and Dixit, A. 2020.** Modelling and analysis of honeycomb sandwich structure using finite element method. *J. Mater. Today*, 25(1): 620-625.
- Zhong, R., Ren, X., Zhang, X. Y., Luo, C., Zhang, Y. and Xie, Y. M. 2022.** Mechanical properties of concrete composites with auxetic single and layered honeycomb structures. *J. Constr. Build. Mater.*, 322(1): 126-153.

Wannarong, D. and Singhanart, T. 2022. Sandwich Composite Structures with 3D Printed Honeycomb Cores. *Mater. Today*, 26(6): 27-39.

B. Simple Books

Gibson, L. J. and Ashby, M. F. 1997. Cellular solids: structure and properties. Press Syndicate of the University of Cambridge, Cambridge, UK. 503 p.

Bitzer, T. N. 1997. Honeycomb technology: materials, design, manufacturing, applications and testing. Springer Science & Business Media, Dordrecht, Netherlands. 230 p.

CURRICULUM VITAE

Name: Amit Kumar Shah

Phone Number: 9917778444

Mailing Address:

Amit Kumar Shah s/o Hari Bhajan Shah,
near Narayan opticals, Srikot,
P.O.- Srinagar Garhwal,
District – Pauri Garhwal,
Uttarakhand (246174)
shahamit844@gmail.com

Permanent Address:

Amit Kumar Shah s/o Hari Bhajan
Shah, near Narayan opticals, Srikot,
P.O.- Srinagar Garhwal,
District – Pauri Garhwal,
Uttarakhand (246174)

Career Objective: To work in field of Simulation analysis.

Educational Qualification:

S. No.	Examination passed	Institution	Year	Percentage/ CGPA
1.	M.Tech.	Govind Ballabh Pant University of Agriculture & Technology, Pantnagar, Uttarakhand	2022	Pursuing
2.	B. Tech.	H. N. B. Garhwal University (A central University), Srinagar Garhwal	2016	67.8
3.	Intermediate	ST. Theresa's Convent School, Srinagar Garhwal	2013	61
4.	High School	ST. Theresa's Convent School, Srinagar Garhwal	2011	61

- **Specialization:** Major: Design and Production Engineering
- **Thesis Title: Modelling and Analysis of Hierarchical Honeycomb Structure using Finite Element Method**
- **Conferences / Seminars / Workshops / Training Attended:** ANSYS Workbench basic to professional Training program from Ardent, Pune. ANSYS Training program from Ardent Computech Private Limited Kolkata, ANSYS workshop by ARK solution Private Limited, Pune.
- **Software skills:** ANSYS, Python, SolidWorks, MS-Office, AutoCAD
- **Professional skill:** Modelling and Static Structural Analysis.

Place: Pantnagar
Date: October, 2022



(Amit Kumar Shah)

Name : Amit Kumar Shah **Id. No.** : 56993
Semester & year of admission : 1st Semester, 2020-2021 **Degree** : M. Tech (Mechanical Engineering)
Major : Design and Production Engineering **Department** : Mechanical Engineering
Thesis Title : **Modelling and Analysis of Hierarchical Honeycomb Structure using Finite Element Method**
No. of pages : 1-58 **Advisor** : Dr. Anadi Misra

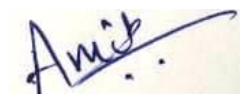
ABSTRACT

Honeycomb structures are strong and light composite structures with a high load bearing capability. A hierarchical honeycomb is a bio-inspired novel honeycomb shape that is employed for structural applications. The stiffness behaviour of hierarchical honeycombs is influenced by superstructure geometry. The deformation of a superstructure-based hierarchical honeycomb with varying cell lengths (4.36 mm, 5.32 mm, 6.28 mm, and 7.14 mm) was investigated in this research. For out of plane directed crushing, a numerical approach using the ANSYS static structure module was applied. The effects of various superstructure geometries were investigated. The boundary condition of a three point bend test configuration was performed on the structure. A deformation force of 200N, 400N, 600N, 800N, and 1000 N was applied at the midpoint of the honeycomb structure's span. The deformation caused in the member reduces as the superstructure cell length rises. The structure gets stiffer and exhibits less deformation as the core height increases. The honeycomb sandwich structure becomes stiffer as the thickness of the face sheet increases. Where weight is not an important structural criterion, a super-structure honeycomb sandwich structure may be the best solution.



(Anadi Misra)

Advisor



(Amit Kumar Shah)

Author

नाम : अमित कुमार शाह परिचायक : ५६९९३
सत्र , प्रवेशवर्ष : प्रथम , २०२०-२०२१ डिग्री : स्नातकोत्तर
मेजर : परिकल्पन और विभाग : यान्त्रिक अभियांत्रिकी
उत्पादान अभियांत्रिकी
शोधशीर्षक : परिमित तत्व विधि का उपयोग करके पदानुक्रमित छत्ते की संरचना
का मॉडलिंग और विश्लेषण
पृष्ठों की संख्या : १-५८ सलाहकार : डॉ अनादि मिश्रा

सारांश

मधुकोश संरचनाएं उच्च भार वहन क्षमता वाली मजबूत और हल्की मिश्रित संरचनाएं हैं। पदानुक्रमित मधुकोश एक जैव-प्रेरित उपन्यास मधुकोश आकार है जो संरचनात्मक अनुप्रयोगों के लिए नियोजित किया जाता है। पदानुक्रमित छत्ते का कठोरता व्यवहार अधिरचना ज्यामिति से प्रभावित होता है। इस शोध में अलग-अलग सेल लंबाई (४.३६ मिमी, ५.३२ मिमी, ६.२८ मिमी, और ७.१४ मिमी) के साथ एक अधिरचना-आधारित पदानुक्रमित छत्ते की विकृति की जांच की गई। आउट ऑफ प्लेन निर्देशित क्रशिंग के लिए, ANSYS स्थिर संरचना मॉड्यूल का उपयोग करते हुए एक संख्यात्मक दृष्टिकोण लागू किया गया था। विभिन्न अधिरचना ज्यामिति के प्रभावों की जांच की गई। संरचना पर तीन बिंदु मोड़ परीक्षण विन्यास की सीमा की स्थिति का प्रदर्शन किया गया था। २००N, ४००N, ६००N, ८००N, और १०००N का विरूपण बल छत्ते की संरचना की अवधि के मध्य बिंदु पर लागू किया गया था। जैसे-जैसे अधिरचना कोशिका की लंबाई बढ़ती है, सदस्य में होने वाली विकृति कम होती जाती है। कोर की ऊंचाई बढ़ने पर संरचना सख्त हो जाती है और कम विरूपण प्रदर्शित करती है। जैसे-जैसे फेस शीट की मोटाई बढ़ती है, मधुकोश सैंडविच की संरचना सख्त होती जाती है। जहां वजन एक महत्वपूर्ण संरचनात्मक मानदंड नहीं है, एक सुपर-स्ट्रक्चर मधुकोश सैंडविच संरचना सबसे अच्छा समाधान हो सकता है।



(डॉ अनादि मिश्रा)
सलाहकार



(अमित कुमार शाह)
लेखक